Design of an indicator to characterize and classify mechanical tests for sheet metals

N. Souto, S. Thuillier, A. Andrade-Campos

Design of an indicator to characterize and classify mechanical tests for sheet metals

N. Souto [a, b], S. Thuillier [b], A. Andrade-Campos [a,*]

[a] *Department of Mechanical Engineering*
Centre for Mechanical Technology and Automation, GRIDS
University of Aveiro, Campus Universitário de Santiago, 3810-193 Aveiro, Portugal

[b] *Univ. Bretagne-Sud, EA4250, LIMATB, F-56100 Lorient, France*

*Corresponding author: gilac@ua.pt (A.Andrade-Campos).

Abstract

The aim of this paper is the design of a quantitative indicator able to distinguish, rate and rank different mechanical tests used to characterize the material behavior of sheet metals. This indicator is formulated considering (i) the strain state range, (ii) the deformation heterogeneity and (iii) the strain level achieved in the test, based on a continuous evaluation of the strain field up to rupture. In order to demonstrate the relevance of the proposed indicator, numerical simulations of classical as well as recent heterogeneous tests were carried out using as input the virtual mechanical behavior of DC04 mild steel. A complex elastoplastic phenomenological model including macroscopic rupture criterion was used. The performance of these tests was compared and their reliability on the mechanical behavior characterization was rated. By using the indicator, a ranking scale ordering the different tests is presented. The obtained results are validated by means of a material parameter sensitivity study. Finally, the proposed indicator can be applied to design new heterogeneous experiments that improve the mechanical characterization of sheet metals and, consequently, material parameter identification.

Keywords: mechanical behavior, strain field, test, heterogeneity, indicator, sheet metal.

1. Introduction

It is well known that the success of finite element (FE) simulations of sheet forming processes is dependent on the quality of input data and, more specifically, on the material parameters associated to the material model adopted. Over the years, material parameters have been identified using classical mechanical tests, such as, uniaxial tension or simple shear, characterized by a rather homogeneous strain distribution over the gauge area of the specimen [1, 2]. This kind of tests provides stress and strain data only for a fixed stress state, being then mandatory to carry out more additional classical tests when the adopted constitutive model depends on the information related to several stress states.

The development of new non-linear constitutive models with larger complexity led to an increase of the number of material parameters to be identified from experiments [3-6]. Thus, it imposes the use of an increasing number of classical tests and, consequently, the material parameters identification process becomes more expensive and time consuming.

Full-field measurement (FFM) methods, that have emerged in the last years (c.f. an overview in Grédiac [7]), directly provide displacement or strain data for all specimen geometry during the test. Such measurements on the overall surface of the specimen became a crucial tool for the analysis of more complex mechanical tests. Indeed, FFM methods overcome the drawback of the strain homogeneity of standard conventional tests by allowing the analysis of heterogeneous tests and monitoring complex strain fields such as the ones observed in real sheet forming processes.

Therefore, heterogeneous experiments aiming at the reproduction of the inhomogeneous and multiaxial strain paths encountered in sheet metal forming processes have been proposed. Most of the heterogeneous experiments available in the literature are based on the modification of (i) classical uniaxial tensile test [8-15] or (ii) biaxial tensile test using a cruciform specimen [16-18]. However, original tests based on a new design of the experiment have also been developed [19-22].

Concerning the geometry of heterogeneous tensile tests, it is mainly designed by (i) adding a hole [15, 16], (ii) notching the specimen [8, 10, 11] or (iii) promoting a shear-like tensile zone [12, 14].

Belhabi *et al*. [8] proposed a non-standard notched tensile test (HTT) for suitable identification of material parameters using FFM method. The specimen consists of a hybrid geometry between the classical tensile test (CTT) and the plane tensile test (PTT) and was designed with the aim of verifying (i) large heterogeneity of the strain in the gauge area, (ii) large strain paths diversity and (iii) good sensitivity of the strain fields to the material parameters. Comparing the tests, the authors verified that HTT presents large diversity of strain paths as well as better sensitivity of the strain fields and concluded that by using heterogeneous experiments, such as HTT, it is expected to identify parameters sets promoting a more reliable prediction of the material behavior.

Pottier *et al*. [15] compared the reliability of the material parameters identified from three different sample geometries. The tests exhibit increasing strain heterogeneities and consist of a classical uniaxial tensile, a tensile with a hole and a shear-like tensile. In order to evaluate the reliability of the three identified parameters sets, numerical simulations of a deep drawing experiment were compared with the experimental data. The results showed that a better numerical reproduction of deep drawing data was obtained with the parameter set identified from the shear-like tensile sample. According to the authors, it leads to the conclusion that the quality of material parameters identified improves and the required number of experiments decreases when the heterogeneity of the strain fields increases.

Nevertheless, since sheet metals undergo multiaxial stressing during forming processes, multiaxial loading experiments are highly desirable for the validation of the plasticity models used in numerical simulations [23]. Hence, it is of great interest to design new configurations for the cruciform specimen used in biaxial testing.

Teaca *et al*. [17] designed two types of cruciform specimens with the aim of obtaining a wide range of strain paths and a high sensitivity to material anisotropy. The specimens were developed in order to use the strain fields measured by a FFM method as input data for material parameter identification. An accurate description of plastic

anisotropy is achievable with this strategy and, consequently, it leads to good predictions of strain distribution, forming limits and springback.

Additionally, Cooreman *et al*. [16] used an identification strategy of material parameters based on a heterogeneous biaxial test. In this work, a perforated cruciform specimen was used and the evaluation of strain field was carried out with digital image correlation (DIC) technique. The authors concluded that a heterogeneous strain field provided much more mechanical information than a homogeneous strain field, leading to a better characterization of the material behavior.

Among the original tests that introduced a new design for the specimen and the loading, the heterogeneous TIX test proposed by Pottier *et al.* [19] must be highlighted. This test is a new testing technique based on out-of-plane motion where the specimen is simultaneously deformed along two perpendicular tensile directions, two perpendicular shear directions and also in expansion, in different areas. This experiment was applied for material parameter identification purposes and, in order to check the quality of the identified parameters, a deep drawing test was carried out. By the comparison of the experimental and numerical results, the authors concluded that a single test can lead to the identification of a complete input parameters set of an anisotropic plastic model.

The above-mentioned works reveal the large benefits of using heterogeneous mechanical tests in the task of parameter identification of material models. Consequently, the design of new heterogeneous tests has been the focus of an increased number of studies.

Nevertheless, no defined criterion yet exists for designing new experiments. In addition, it is rather difficult to compare heterogeneous tests (or even heterogeneous and classical tests) and define the best one for the characterization of the material behavior. Therefore, it is crucial to determine if a given mechanical test provides more information, as well as with a higher reliability, for the characterization of the material behavior than another test. In this way, it will be possible to achieve the current aims for the mechanical characterization of sheet metals: (i) identify large sets of material parameters, (ii) improve the quality of the identified parameters and (iii) reduce the number of required experimental tests.

Therefore, the problem of ranking the information provided by the tests and of choosing the most suitable test for parameter identification is still unsolved. For this reason, the main goal of this work is the design of a quantitative indicator able to distinguish and rate different mechanical tests. The purpose of this indicator is also to guide the design process of new heterogeneous tests. In this way, a more straightforward, efficient and successful development of new mechanical tests can be achieved. The indicator can be used to compare new designs of tests with other existent tests and to query its reliability on the material behavior characterization of sheet metals.

Thereby, the formulation of an indicator focused on the mechanical behavior of sheet metal is presented and applied considering classical as well as heterogeneous tests. With the aim of validating the results obtained by the proposed indicator, an analysis of the material parameter sensitivity [8] for the chosen tests was performed.

2. Design of the indicator

In order to properly formulate the indicator, it is mandatory to define a list of the main features and mechanical phenomena presented in sheet metal forming that should be covered. Only in this way, will it be possible to design a quantitative indicator able to show that one mechanical test is more informative than another one. It must be noted that a mechanical test is considered more informative if a larger number of mechanical phenomena and stress/strain states are covered. Hence, the indicator must be an evaluation criterion rating the difference between tests and should include the following aims:

- Recognize and quantify all distinct strain states presented in the mechanical test, favoring tests that cover larger strain state range with a minor number of gaps.
- Analyze the deformation heterogeneity of the specimen during the test, promoting tests with large non-homogeneity.
- Evaluate the maximum strain achieved for the most important strain states, promoting the increase of these values.

- Quantify the average strain level, taking into account the geometry, and favoring large values of this average strain.
- Promote a continuous evaluation of the test up to rupture.
- Promote the unicity of the solution when identification strategies are used.

The listed features should be quantified to define the indicator and must be continuously evaluated during the test up to rupture. These can be arranged in the following two groups: (i) strain state range and heterogeneity and (ii) strain level.

The mechanical information conveyed by a test can be fully described by the strain and stress states. However, in order to be calculated both from experimental and numerical results, the indicator is solely based on information related to the strain state and stress invariants such as the equivalent stress, triaxiality ratio and Lode parameter were not considered in this work.

2.1. Features of the indicator

2.1.1 Strain state range and heterogeneity

As previously pointed out, several strain states are expected during sheet metal forming processes. Due to this reason, the strain state range of the test must be taken into account by the indicator. According to the continuum mechanics theory, a progressive deformation takes place continuously. Therefore, the strain state range of the mechanical test can be evaluated by the maximum and minimum strain state values achieved in the test. To accomplish this, the ratio between the minor ε_2 and major ε_1 principal strains is considered since it can distinguish different strain states, as depicted in Fig. 1. Therefore, the strain state range covered $(\varepsilon_2/\varepsilon_1)_R$ is measured by using the minimum and maximum $\varepsilon_2/\varepsilon_1$ values obtained in the test and is given by,

$$\left(\frac{\varepsilon_2}{\varepsilon_1}\right)_R = \left(\frac{\varepsilon_2}{\varepsilon_1}\right)_{max} - \left(\frac{\varepsilon_2}{\varepsilon_1}\right)_{min}. \quad (1)$$

However, $(\varepsilon_2/\varepsilon_1)_R$ may not be able to characterize fully the strain state range information. Indeed, the diversity of the mechanical information obtained by the strain

state range is not characterized by Eq. 1, since large strain state bounds do not necessarily means large diversification of the mechanical information provided by the test. A practical example of this situation consists in the conventional simple shear test using rectangular specimen. Indeed, most part of the specimen region corresponds to a simple shear strain state ($\varepsilon_2/\varepsilon_1 = -1$) and the remaining small region near the free edges exhibits distinct strain states (tension and compression) [24]. Nevertheless this test can be considered as quasi-homogeneous within the central area. In this way, the diversification of the mechanical information given by the test is a relevant feature that must be considered and can be evaluated measuring the strain state range variation of the specimen during the test. In this work, the strain state range variation of the test is determined by the standard deviation (*Std*) of $\varepsilon_2/\varepsilon_1$ values obtained for the specimen during the test. Note that *Std* is a statistical function that shows how much dispersion from the average exists. A low *Std* value indicates that the data points tend to be very close to the mean (which is the case for homogeneous experiments) while a high *Std* value indicates that the data points are spread out over a large range of values, expected for heterogeneous tests.

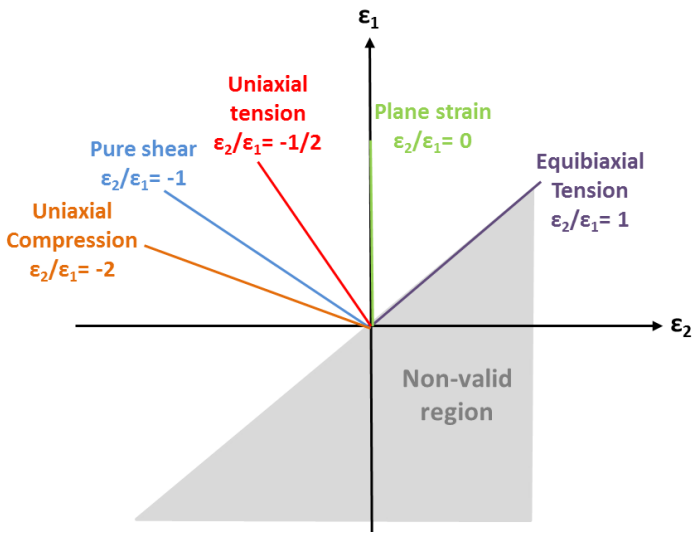

Fig. 1. Range of $\varepsilon_2/\varepsilon_1$ values of the most relevant strain states observed in sheet metal forming, considering material isotropy.

Histograms representing $\varepsilon_2/\varepsilon_1$ distribution of subareas of the sample or the elements of the meshed specimen, when using DIC measurements or FEM analysis, respectively, are an easy way to visualize the applicability of $Std(\varepsilon_2/\varepsilon_1)$. $Std(\varepsilon_2/\varepsilon_1)$ is defined as

$$Std\left(\frac{\varepsilon_2}{\varepsilon_1}\right) = \sqrt{\frac{\sum_i^n [(\varepsilon_2/\varepsilon_1)_i - \mu_{\varepsilon_2/\varepsilon_1}]^2}{n-1}}, \quad (2)$$

where $(\varepsilon_2/\varepsilon_1)_i$ is the ratio $\varepsilon_2/\varepsilon_1$ for subarea or element i of the mesh, $\mu_{\varepsilon_2/\varepsilon_1}$ is the mean value of $\varepsilon_2/\varepsilon_1$ of the specimen and n is the number of elements or subareas. Fig. 2 shows two histograms with distinct $\varepsilon_2/\varepsilon_1$ distributions. In both cases, the same strain state range is covered. However, the diversity of the mechanical information provided differs. A large distribution of element sets with similar number of elements in each set corresponds to a high diversity of the mechanical information giving high $Std(\varepsilon_2/\varepsilon_1)$, since a large quantity of elements is far to $\mu_{\varepsilon_2/\varepsilon_1}$ (Fig. 2 a)). On the contrary, when the majority of the elements presents similar $\varepsilon_2/\varepsilon_1$ values, a lower $Std(\varepsilon_2/\varepsilon_1)$ for the test is obtained since the majority of the elements is close to $\mu_{\varepsilon_2/\varepsilon_1}$ (Fig. 2 b)).

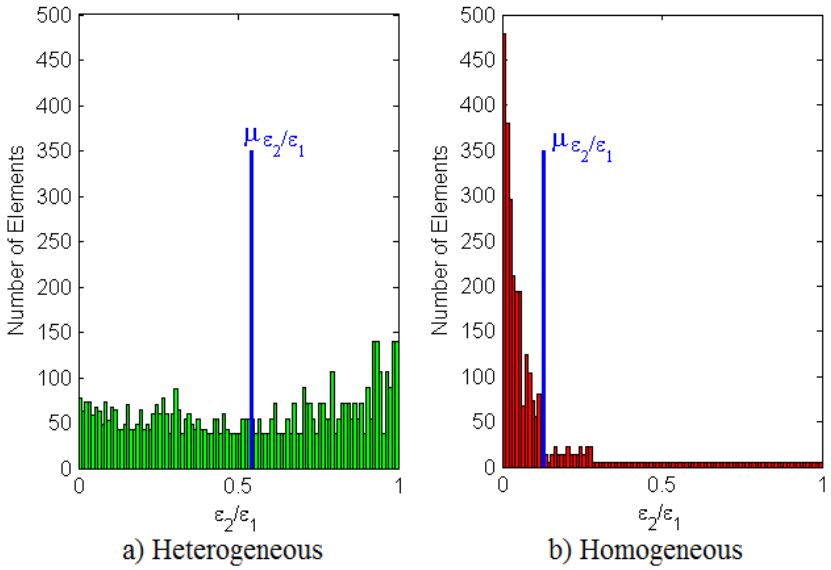

Fig. 2. Histograms representing $\varepsilon_2/\varepsilon_1$ distribution in finite subareas or elements in the specimen. $\mu_{\varepsilon_2/\varepsilon_1}$ corresponds to average $\varepsilon_2/\varepsilon_1$ value.

Additionally, it is well known that the non-homogeneity of the specimen deformation is also a crucial factor for the larger diversification of the mechanical information of the test. Therefore, the deformation heterogeneity of the specimen is also taken into account in the formulation of the indicator. In that respect, the non-homogeneity of the strain field during the test is evaluated through the variation of the equivalent plastic strain ($\bar{\varepsilon}^P$) by assessing $Std(\bar{\varepsilon}^P)$, such as

$$Std\left(\bar{\varepsilon}^{\mathrm{P}}\right)=\sqrt{\frac{\sum_{i}^{n}\left(\bar{\varepsilon}_{i}^{\mathrm{P}}-\bar{\varepsilon}^{\mathrm{P}}\right)^{2}}{n-1}}, \tag{3}$$

where $\bar{\varepsilon}_{i}^{\mathrm{P}}$ is the equivalent plastic strain of the specimen subarea or element *i* and $\bar{\varepsilon}^{\mathrm{P}}$ is the mean $\bar{\varepsilon}^{\mathrm{P}}$ value of the sample.

2.1.2 Strain level

One of the main goals considered in the development of tests for material parameter identification is to reach the same deformation level as the one recorded in sheet metal forming processes. Hence, the maximum strain ($\bar{\varepsilon}_{\mathrm{Max}}^{\mathrm{P}}$) achieved on the test is a crucial data that must be evaluated by the indicator. $\bar{\varepsilon}_{\mathrm{Max}}^{\mathrm{P}}$ is calculated taking into account the maximum $\bar{\varepsilon}^{\mathrm{P}}$ values obtained (i) for the test as well as (ii) for the most relevant strain states (namely, equibiaxial tension, pure shear, uniaxial tension, plane strain tension and uniaxial compression) and can be written as

$$\bar{\varepsilon}_{\mathrm{Max}}^{\mathrm{P}}=\frac{\bar{\varepsilon}_{\mathrm{test}}^{\mathrm{P}}+\bar{\varepsilon}_{\mathrm{tens}}^{\mathrm{P}}+\bar{\varepsilon}_{\mathrm{shear}}^{\mathrm{P}}+\bar{\varepsilon}_{\mathrm{biaxial}}^{\mathrm{P}}+\bar{\varepsilon}_{\mathrm{comp}}^{\mathrm{P}}+\bar{\varepsilon}_{\mathrm{plane}}^{\mathrm{P}}}{6}. \tag{4}$$

Note that Eq. 4 is defined by giving equal importance to each term and, then, $\bar{\varepsilon}_{\mathrm{Max}}^{\mathrm{P}}$ consists of a mean value of the maximum $\bar{\varepsilon}^{\mathrm{P}}$ values. It was considered that any strain state is not more relevant than the other ones, including also the test condition. It is rather difficult to assume that, for example, uniaxial tension is more important than simple shear and, consequently, to attribute different weight for these strain states. Actually, from a strain state point of view, uniaxial tension and simple shear are complementary since the first one only involves diagonal components of the strain tensor while the second one involves non-diagonal components of the strain tensor. Furthermore, gathering all these terms avoids to have several individual contributions in

the indicator formulation and also allows to easily normalize the indicator contribution of Eq. 4.

Additionally, the average deformation obtained in the specimen is also considered on the definition of the indicator since this feature points out the global level of deformation imposed during the test. Larger values of average deformation contribute to a more informative test. The average deformation ($Av_{\bar{\varepsilon}^{\mathrm{P}}}$) of the test is calculated by

$$Av_{\bar{\varepsilon}^{\mathrm{P}}} = \frac{\sum_i^n \bar{\varepsilon}_i^{\mathrm{P}} v_i}{v_{\mathrm{T}}}, \tag{5}$$

where v_{i} is the volume of the element or subarea i and v_{T} is the total volume of the specimen. Note that, in order to normalize the average deformation to the specimen geometry, $Av_{\bar{\varepsilon}^{\mathrm{P}}}$ is defined accounting for the volume of the specimen. In this way, $Av_{\bar{\varepsilon}^{\mathrm{P}}}$ values of tests with different specimen geometry can be compared.

2.2. Mathematical formulation

The indicator is formulated based on Eqs. 1-5 which characterize the strain state range and heterogeneity as well as strain level features. However, some considerations must be taken into account for its formulation.

For instance, in some tests, plastic instabilities can occur before achieving rupture and these phenomena may provide useful additional information for a better characterization of the material behavior. For this reason, the indicator must be based on a continuous evaluation of the strain field up to rupture. To this end, a macroscopic rupture criterion is used in order to stop the numerical simulation when the criterion is reached.

Within the characterized features, $\bar{\varepsilon}^{\mathrm{P}}_{\mathrm{Max}}$ and $Av_{\bar{\varepsilon}^{\mathrm{P}}}$ consist of cumulative data of the test. As a result, just the values obtained at the end of the test are considered on the indicator calculation.

Nevertheless, $(\varepsilon_2/\varepsilon_1)_R$, $Std(\bar{\varepsilon}^P)$ and $Std(\varepsilon_2/\varepsilon_1)$ are not cumulative and may change in subsequent increments of the test mostly due to the heterogeneity. As a consequence, the mean values of $Std(\bar{\varepsilon}^P)$ and $Std(\varepsilon_2/\varepsilon_1)$ calculated over the all test time are considered in the definition of the indicator. Nonetheless, in the case of $(\varepsilon_2/\varepsilon_1)_R$, just the value obtained at the end of the test is taken into account. This is justified by the fact that $(\varepsilon_2/\varepsilon_1)_R$ is dependent of the heterogeneity and, generally, the large heterogeneity of the test occurs at rupture.

By considering the previous assumptions, the proposed indicator I_T is defined as

$$I_T = w_{r1}\frac{\mathrm{Mean}\left(\mathrm{Std}\left(\varepsilon_2/\varepsilon_1\right)\right)}{w_{a1}} + w_{r2}\frac{\left(\varepsilon_2/\varepsilon_1\right)_R}{w_{a2}} + w_{r3}\frac{\mathrm{Mean}\left(\mathrm{Std}\left(\bar{\varepsilon}^P\right)\right)}{w_{a3}} + w_{r4}\frac{\bar{\varepsilon}^P_{Max}}{w_{a4}} + w_{r5}\frac{Av_{\bar{\varepsilon}^P}}{w_{a5}}, \quad (6)$$

where w_r and w_a are relative and absolute weighting factors. Table 1 shows w_r and w_a values adopted in this work.

Table 1. Weighing factors used on the definition of I_T.

w_{a1}	w_{a2}	w_{a3}	w_{a4}	w_{a5}
1	4	0.25	1	1
w_{r1}	w_{r2}	w_{r3}	w_{r4}	w_{r5}
0.3	0.03	0.17	0.4	0.1

The absolute weighting factors w_a have physical meaning and correspond to the maximum achievable value for each indicator term. The weights w_{a4} and w_{a5} were defined assuming that the maximum and average $\bar{\varepsilon}^P$ values that can be obtained in the test are 1. Concerning w_{a1} and w_{a3}, these absolute weighting factors were selected based on the mean values of $Std(\bar{\varepsilon}^P)$ and $Std(\varepsilon_2/\varepsilon_1)$ obtained for the different tests considered in this work (Section 3). In the case of w_{a2}, this one is defined limiting the strain state range between equibiaxial state ($\varepsilon_2/\varepsilon_1$=1) and a compression state presenting $\varepsilon_2/\varepsilon_1$=-3, therefore, w_{a2}=4. It must be noted that in the case of a uniaxial compression strain state for material isotropy, $\varepsilon_2/\varepsilon_1$= -2, as illustrated by Fig. 1. However, it was defined to evaluate a broader strain state range $(\varepsilon_2/\varepsilon_1)_R$. These bounds are imposed to the numerical

analysis of $(\varepsilon_2/\varepsilon_1)_R$ since high negative values can be obtained, as can be seen in Fig. 1. Moreover, the main strain states are covered by this range and in sheet metal forming it is not expected to obtain relevant compression states, due to buckling. The purpose of w_a factors is to normalize each term of the indicator, which is useful for evaluating the indicator contributions.

The relative weighting factors w_r can be defined by the user taking into account the importance attributed to each I_T contribution and must be considered in order to (i) scale, for any mechanical test, the indicator value between 0 and the unity and (ii) adjust the importance of each term on the calculation of the indicator. Note that, though each indicator term defines a different feature, some of these features are related. Thus, relative weighting factors are needed for defining the importance of each I_T term considering the inherent relation between some of the indicator features. The focus of these w_r factors is adjusting the contributions of each one of the indicator terms aiming a proper calculation of I_T. For this purpose, w_r factors were defined attributing equal importance to the contributions of both strain state range/heterogeneity ($w_{r1}+w_{r2}+w_{r3}=0.5$) and strain level ($w_{r4}+w_{r5}=0.5$) groups. According to this, the several w_r values listed in Table 4 were adjusted empirically taking into account the order of magnitude estimated from the numerical simulation of the mechanical tests considered in this work (Section 3). This standard choice seems a reasonable decision for the calculation of I_T, considering the inherent relation between some of the indicator features of each group as well as that one group is not favored relatively to the other one. Additionally, for scaling the indicator value between 0 and the unity, the sum of the several w_r values is equal to 1.

It must be stressed out that the proposed indicator may be calculated from both real (experiments) as well as virtual (numerical simulation) tests. For that, it is just necessary take into account a different definition of $\bar{\varepsilon}^P$ for the experimental data provided by DIC measurements, since the numerical $\bar{\varepsilon}^P$ is associated to the constitutive model adopted. The application of this indicator mainly concerns mechanical tests involving thin metallic sheets used in metal forming.

3. Numerical test evaluation

3.1. Presentation of the tests

Several tests were considered for evaluating the proposed indicator: (i) uniaxial tensile test [25], (ii) simple shear test [26], (iii) equibiaxial bulge test [27], (iv) classical biaxial test using cruciform specimen [28], (v) plane strain test [29], (vi) TIX test [19], (vii) biaxial tensile test using a perforated cruciform sample [17] and (viii) tensile test using a shear-like tensile specimen [11].

The reason for such a selection is the fact that they reproduce different types of stress/strain states. Additionally, it must be highlighted that these tests consist of classical or quasi-homogeneous (i,…,v) as well as heterogeneous experiments (vi,…,viii) and their performance characterizing the material behavior can be compared. Indeed, by calculating I_T for each test it was possible to establish a ranking, hence rating the importance of each one. This analysis allows inquire for the most informative test among the selected ones. Figs. 3 and 4 show, respectively, the specimen geometries of the classical and heterogeneous tests. It must be noticed that the plane strain specimen proposed in [29] only promotes near-plane strain tension. Thereby, in order to obtain a more accentuated plane strain state for this test, the width of the plane strain specimen was increased up to 285 mm (Fig. 3 d)).

TIX test [19], depicted in Fig. 4 a), is based on the use of a uniaxial tensile device with a specimen subjected to out-of-plane motion carried out by a hemispherical punch with a diameter of 15 mm. The vertical displacement is applied at the center of the specimen while the specimen is tightly pinned between the die and the holder. The specimen has a circular shape with a diameter of 100 mm and grooves were machined. This geometry exhibits highly heterogeneous strain paths allowing the reproduction of tension and shear at 0° (RD) and 90° (TD) to the rolling direction and also expansion in the central part of the sample, as well as an out-of-plane displacement.

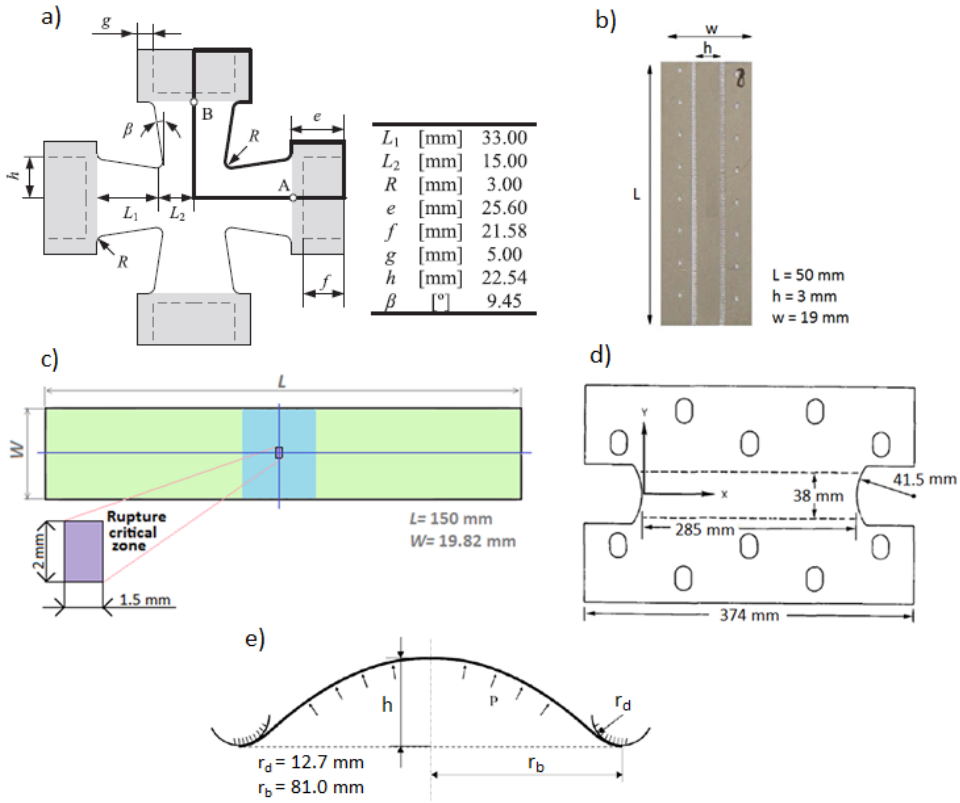

Fig. 3. Classical a) biaxial tensile, b) simple shear, c) uniaxial tensile, d) plane strain tension and e) bulge test.

The shear-like tensile test [11] illustrated in Fig. 4 b) consists of a tensile test carried out using a non-standard sample. This sample was designed with a shear-like tensile zone in order to provide both tensile and shear strain data.

The heterogeneous biaxial tensile test on non-standard perforated cruciform specimen, shown in Fig. 4 c), was designed for obtaining high sensitivity of strain fields to material anisotropy. This test was used to characterize the material behavior for deformation paths composed by the stress range from uniaxial to plane strain tension [17].

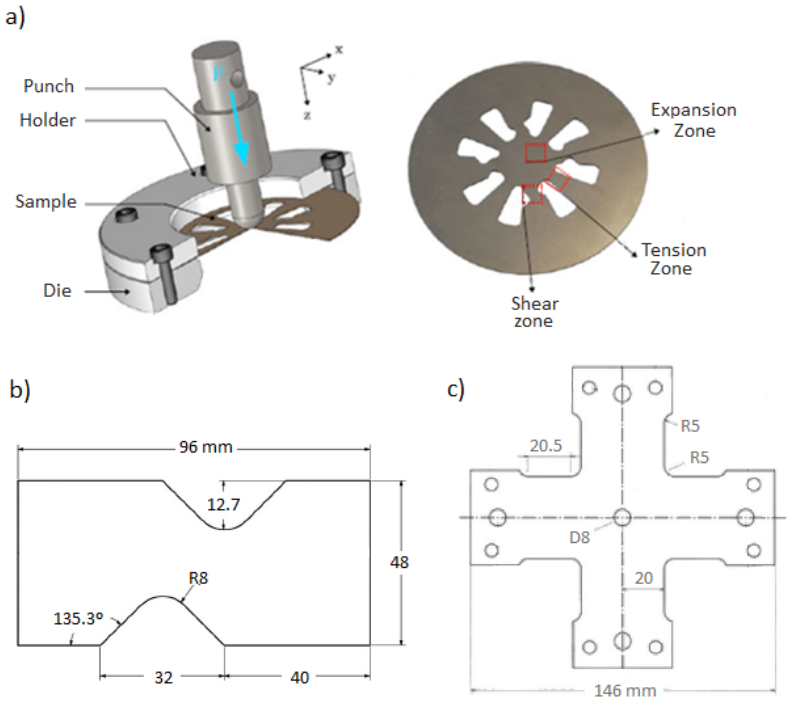

Fig. 4. Heterogeneous a) TIX b) shear-like tensile and c) biaxial tensile test using perforated cruciform sample.

3.2. Constitutive model and rupture criterion

The numerical simulations of the tests were carried out using the virtual behavior of DC04 mild steel. The anisotropy and hardening behavior of this steel was reproduced by using a complex phenomenological model composed by the non-quadratic *Yld2004-18p* yield criterion combined with a mixed isotropic-kinematic hardening law. In addition, the rupture behavior was characterized by the calibration of Cockroft and Latham (CL) fracture criterion. The detailed description of the material model adopted as well as the input material parameters characterizing this DC04 mild steel can be found in [25]. A summary of the constitutive formulations is given in Table 2.

Table 2. Constitutive formulations.

Isotropic hardening:	$\sigma_{\mathrm{Y}}(\bar{\varepsilon}^{\mathrm{P}}) = \sigma_0 + (\sigma_\infty - \sigma_0)\left[1 - \exp(-\delta\bar{\varepsilon}^{\mathrm{P}})\right] + \beta\bar{\varepsilon}^{\mathrm{P}}$
Kinematic hardening:	$\dot{\boldsymbol{\alpha}} = \sum_{i=1}^{3}\left(\frac{C_i}{\bar{\eta}}\boldsymbol{\eta} - \gamma_i\boldsymbol{\alpha}\right)\dot{\bar{\varepsilon}}^{\mathrm{P}}$
Yld2004-18p yield criterion:	$\bar{\eta}(\boldsymbol{\eta}) = \sum_{i=1,j=1}^{3}\left\lvert\tilde{\mathbf{S}}_i^{(1)} - \tilde{\mathbf{S}}_j^{(2)}\right\rvert^a = 4\sigma_{\mathrm{Y}}{}^a$
	$\tilde{\mathbf{S}}^{(k)} = \tilde{\mathbf{L}}^{(k)} : \mathbf{S}, \quad k = 1,2$
	$\tilde{\mathbf{L}}^{(k)} = \begin{bmatrix} 0 & -c_{12}^{(k)} & -c_{13}^{(k)} & 0 & 0 & 0 \\ -c_{21}^{(k)} & 0 & -c_{23}^{(k)} & 0 & 0 & 0 \\ -c_{31}^{(k)} & -c_{32}^{(k)} & 0 & 0 & 0 & 0 \\ 0 & 0 & 0 & c_{44}^{(k)} & 0 & 0 \\ 0 & 0 & 0 & 0 & c_{55}^{(k)} & 0 \\ 0 & 0 & 0 & 0 & 0 & c_{66}^{(k)} \end{bmatrix}$
CL fracture criterion:	$W = \int_0^{\bar{\varepsilon}_{\mathrm{P}}^{\mathrm{f}}} \frac{\sigma_I}{\bar{\sigma}} \mathrm{d}\bar{\varepsilon}^{\mathrm{P}} \leq W_{\mathrm{CL}}$

3.3. Numerical modeling

The computational analysis was carried out considering implicit time integration scheme by using Abaqus/Standard FE code. The tests were modeled with 3D 8-node linear isoparametric elements with reduced integration (C3D8R) and with hourglass control. Symmetry conditions were used for uniaxial tensile, bulge, biaxial tensile and plane strain tension tests in order to reduce the computational time. Only one fourth of uniaxial tensile (symmetry in the thickness and width), bulge and biaxial tensile geometries were modeled while half specimen was considered in the case of plane strain test. Fig. 5 shows the boundary conditions for all the tests. It must be mentioned that the punch of TIX test was defined as an analytical rigid surface and the lubrication coefficient taken into account was 0.25, as suggested in [19].

The constitutive model was introduced as a user-defined material subroutine (UMAT) in the FE commercial code ABAQUS. A mesh density of 3 elements/mm was used for all the tests. Additionally, samples were meshed with 3 elements along the

thickness. The specimens of the several mechanical tests were defined with a thickness of 0.7 mm. This thickness value is the same of DC04 mild steel sheet used for identifying the material parameters of the constitutive model chosen.

The analysis of the tests for calculating I_T was carried out considering the evaluation of the specimen surface. Such as in DIC technique, a region of interest (ROI) of the sample was defined and the strain field was measured only in this region. In the case of uniaxial tensile, plane strain tension, shear-like tensile and biaxial tensile tests, all the deformed geometry was taken into account. However, for simple shear, bulge and TIX tests, a ROI was defined to avoid local effects such as the contact with the tools or to avoid regions that cannot be measured experimentally by FFM methods. These ROI are illustrated in Fig. 5 as red zones.

Concerning $\varepsilon_2/\varepsilon_1$ analysis, this ratio was accurately defined by calculating the eigenvalues and eigenvectors for each finite element in order to determine accurately the major ε_1 and minor ε_2 principal strains in the sheet plane. A python script was developed to perform the $\varepsilon_2/\varepsilon_1$ analysis in post-processing, after the numerical simulation. $\varepsilon_2/\varepsilon_1$ ratio was only determined for elements exhibiting a certain amount of equivalent plastic strain *i.e.*, with $\bar{\varepsilon}^{P} \geq 1\text{x}10^{-3}$. The values of $(\varepsilon_2/\varepsilon_1)_{max}$ and $(\varepsilon_2/\varepsilon_1)_{min}$ were identified from the sample zones with higher and lower $\varepsilon_2/\varepsilon_1$ ratio, taking into account that the lower admissible $\varepsilon_2/\varepsilon_1$ ratio for I_T calculation is -3.

Relatively to $\bar{\varepsilon}^{P}$ values obtained for the test as well as for the most relevant strain states, it must be pointed out that $\bar{\varepsilon}^{P}_{test}$ is calculated as an average over the 15 elements (region with approximately 1.5x1 mm^2) with highest $\bar{\varepsilon}^{P}$ value while $\bar{\varepsilon}^{P}$ of the different strain states is calculated as the average value for all elements having $\varepsilon_2/\varepsilon_1$ range depicted in Table 3. Note that due to DC04 material anisotropy, $\varepsilon_2/\varepsilon_1$ values characterizing uniaxial tensile and uniaxial compression states of DC04 mild steel are -0.627 and -1.595, respectively.

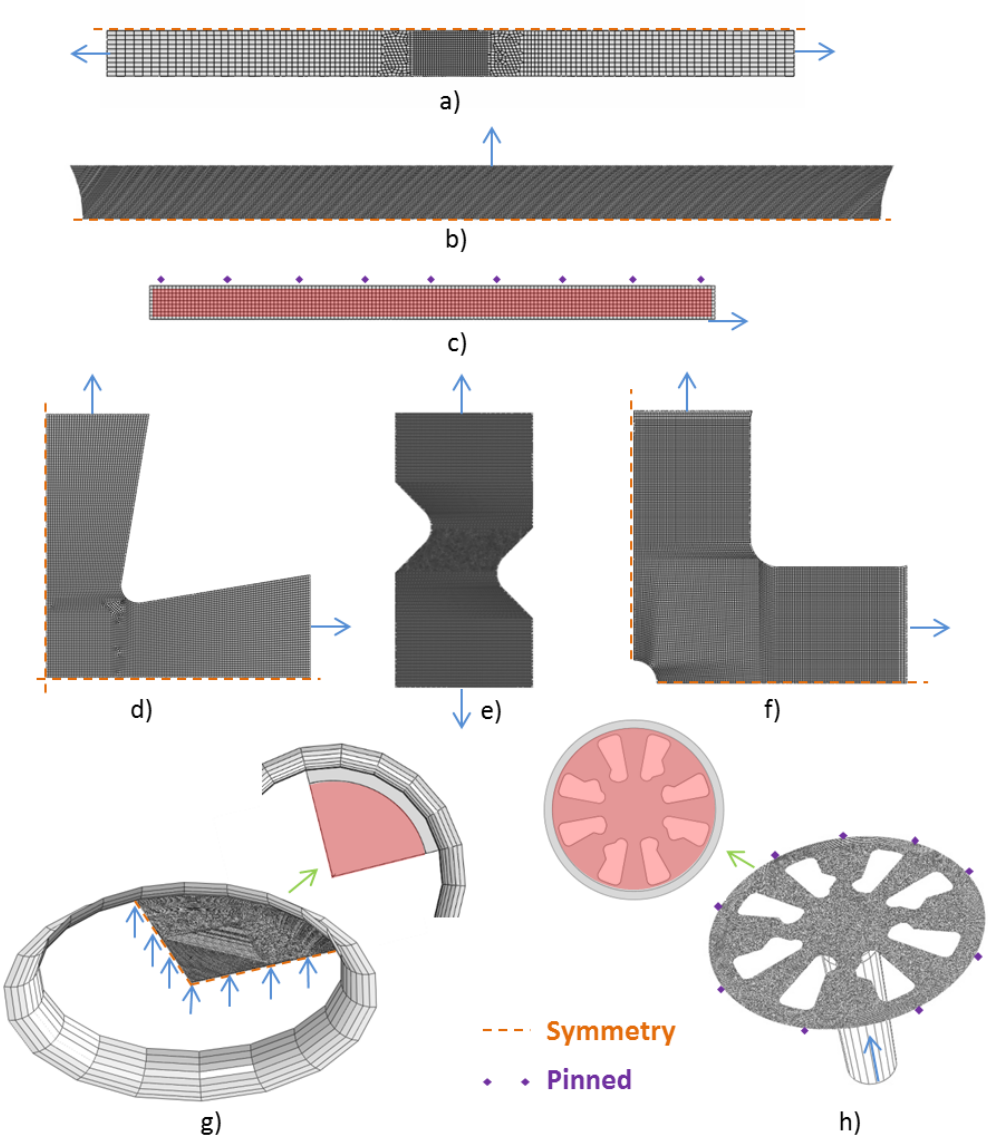

Fig. 5. Numerical model of a) uniaxial tensile, b) plane strain tension, c) simple shear, d) classical biaxial tensile, e) shear-like tensile, f) biaxial tensile with hole, g) bulge and h) TIX test.

Table 3. $\varepsilon_2/\varepsilon_1$ range characterizing the different strain states considered for I_T calculation.

Strain State	$\varepsilon_2/\varepsilon_1$ range
Uniaxial tension	-0.627 ± 0.03
Shear	-1 ± 0.03
Plane strain tension	0 ± 0.03
Equibiaxial	1 (0.94 - 1)
Uniaxial compression	-1.595 ± 0.03

4. Results and discussion

The different terms used in I_T formulation are analysed for the several tests. The calculation of I_T and its robustness to variation of the relative weighting factors are also presented in this section.

4.1. Calculation of I_T

With the aim of obtaining a visual description of $\bar{\varepsilon}^P$ evolution during the test, histograms showing $\bar{\varepsilon}^P$ distribution at normalized times 0.5, 0.75 and 1 (end of the test) are depicted in Figs. 6 and 7. The histograms represent $\bar{\varepsilon}^P$ distribution on element sets divided in 100 equal intervals. By the analysis of these element sets it is possible to analyze the level of heterogeneity of each test since the distribution of elements sets is directly proportional to the deformation heterogeneity of the specimen. Large element set distribution with a similar number of elements and, consequently, heterogeneity is verified for biaxial tensile tests using classical cruciform specimen and also perforated sample, as can be seen in Figs. 6 d) and 7 c). On the contrary, a narrow distribution of element sets composed of a high number of elements indicates non-heterogeneity, as observed in the case of uniaxial tensile, TIX and shear-like tensile tests before strain localization (histograms at times t=0.5 and t=0.75) illustrated, respectively, in Figs. 6 a), 7 b) and 7 d). It must be highlighted that TIX and shear-like tensile are heterogeneous tests, however, their heterogeneity occur in small areas of the ROI.

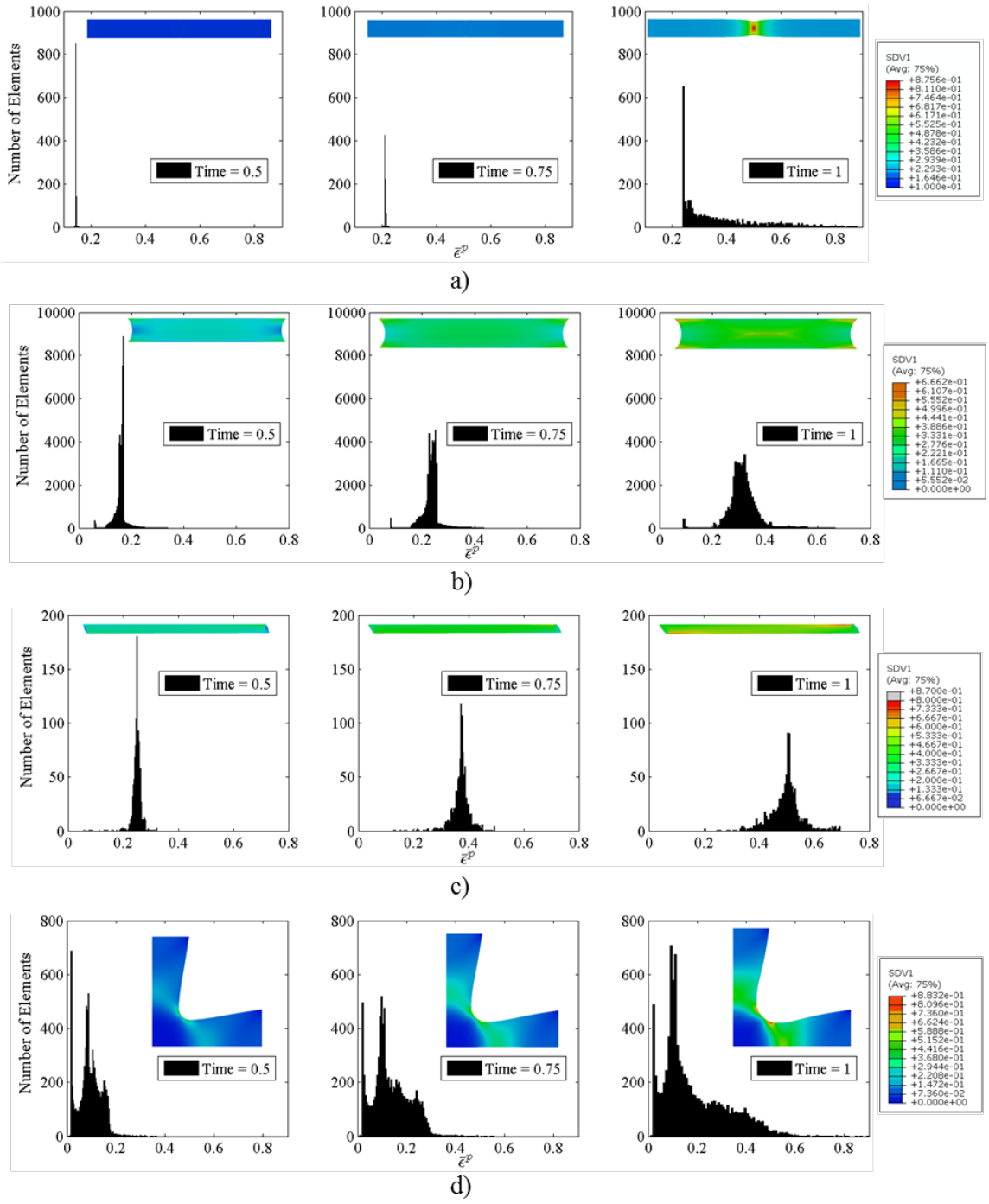

Fig. 6. Histograms representing $\bar{\varepsilon}^{\mathrm{P}}$ distribution of the elements for a) uniaxial tensile, b) plane strain tension, c) simple shear and d) classical biaxial tensile test. SDV1 stands for $\bar{\varepsilon}^{\mathrm{P}}$.

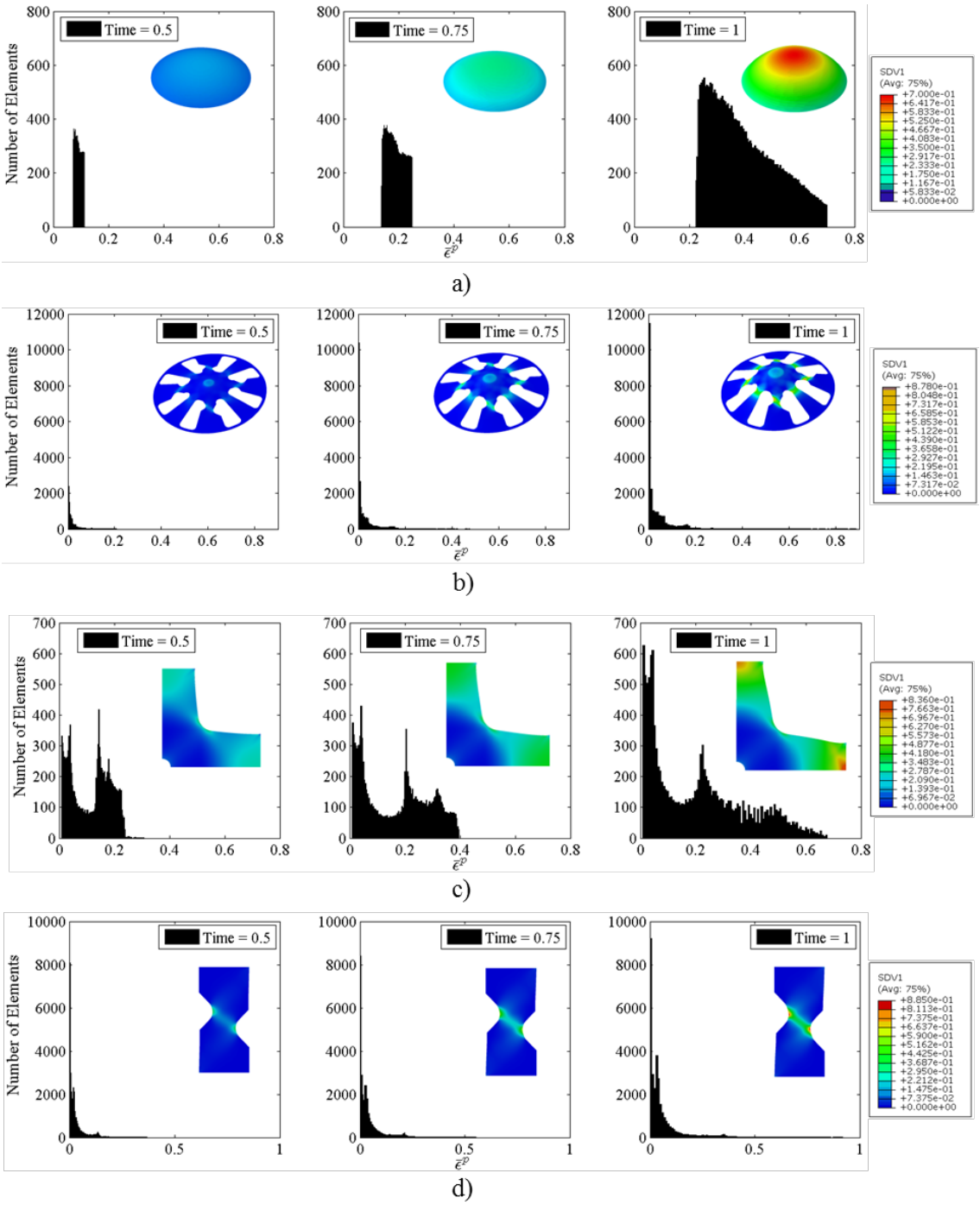

Fig. 7. Histograms representing $\bar{\varepsilon}^{P}$ distribution of the elements for a) bulge, b) TIX, c) biaxial with hole and d) shear-like tensile test. SDV1 stands for $\bar{\varepsilon}^{P}$.

Note that accurate $\bar{\varepsilon}^{P}$ distributions using histograms are only possible considering a constant element size for the all mesh. Otherwise, element sets would not represent equally the area of the specimen.

Additionally, $\bar{\varepsilon}^{P}$ specimen distribution is presented in Figs. 6 and 7. These contours show the location of the heterogeneity regions as well as $\bar{\varepsilon}^{P}$ value obtained on the sample.

Similarly, histograms reproducing $\varepsilon_2/\varepsilon_1$ distribution on the specimen during the test as well as $\varepsilon_2/\varepsilon_1$ contours were analyzed, as shown in Figs. 8 and 9. These figures show that $\varepsilon_2/\varepsilon_1$ range covered by each test is almost constant during the experiment since no significant changes occur on the element set distribution. The tests that present some smooth $\varepsilon_2/\varepsilon_1$ range variation between half time and the end of the test are the uniaxial tensile and the bulge test. The strain state range of the uniaxial tensile test is comprised between $-0.64 < \varepsilon_2/\varepsilon_1 < -0.62$ before strain localization (t=0.5~0.75) and after necking phenomenon the strain state range covered is $-0.64 < \varepsilon_2/\varepsilon_1 < -0.54$ (t=1), as shown in Fig. 8 a). Taking into account that the strain state range evaluation is performed in-between $-3 \leq \varepsilon_2/\varepsilon_1 \leq 1$, the increase of $\varepsilon_2/\varepsilon_1$ range observed in uniaxial tensile test is not substantial.

The larger is the strain range covered, the larger is the diversity of the mechanical state information given by the test. As expected, classical tests such as uniaxial tensile, simple shear or bulge test provide mainly uniaxial tensile ($\varepsilon_2/\varepsilon_1$=-0.627), shear ($\varepsilon_2/\varepsilon_1$=-1) and equibiaxial ($\varepsilon_2/\varepsilon_1$=1) strain states, as can be seen in Figs. 8 a), 8 b) and 9 a), respectively. However, several strain states are covered by biaxial tensile tests using classical cruciform specimen or perforated sample (Figs. 8 d) and 9 c)), TIX test (Fig. 9 b)) and shear-like tensile test (Fig. 9 d)).

In the case of biaxial tensile test using classical cruciform sample (Fig. 8 d)), strain state range between uniaxial and equibiaxial tensions is characterized. Hence, plane strain state ($\varepsilon_2/\varepsilon_1$=0) is also included in this test. A similar $\varepsilon_2/\varepsilon_1$ range is achieved using the perforated cruciform sample (Fig. 9 c)). It should be noted that the test is similar, however, the hole at the center of the sample hinders the propagation of the biaxial strain state. Thereby, this strain state is localized in small regions of the specimen, as shown by $\varepsilon_2/\varepsilon_1$ contour. Concerning shear-like tensile test, it is possible to see in Fig. 9 d) that this test exhibits uniaxial compressive and tensile strain states. A large $\varepsilon_2/\varepsilon_1$ range is covered by this test comparatively to the uniaxial tensile test (Fig. 8 a)). However, the covered $\varepsilon_2/\varepsilon_1$ strain range is not continuous due to the observed gap

between compressive and tensile state. It results not only from the specimen design but also from the imposed condition to determine $\varepsilon_2/\varepsilon_1$ ratio only for elements with $\bar{\varepsilon}^P \geq 1x10^{-3}$ as well. Consequently, grey regions on $\varepsilon_2/\varepsilon_1$ contour of shear-like tensile test means that the imposed condition was not satisfied.

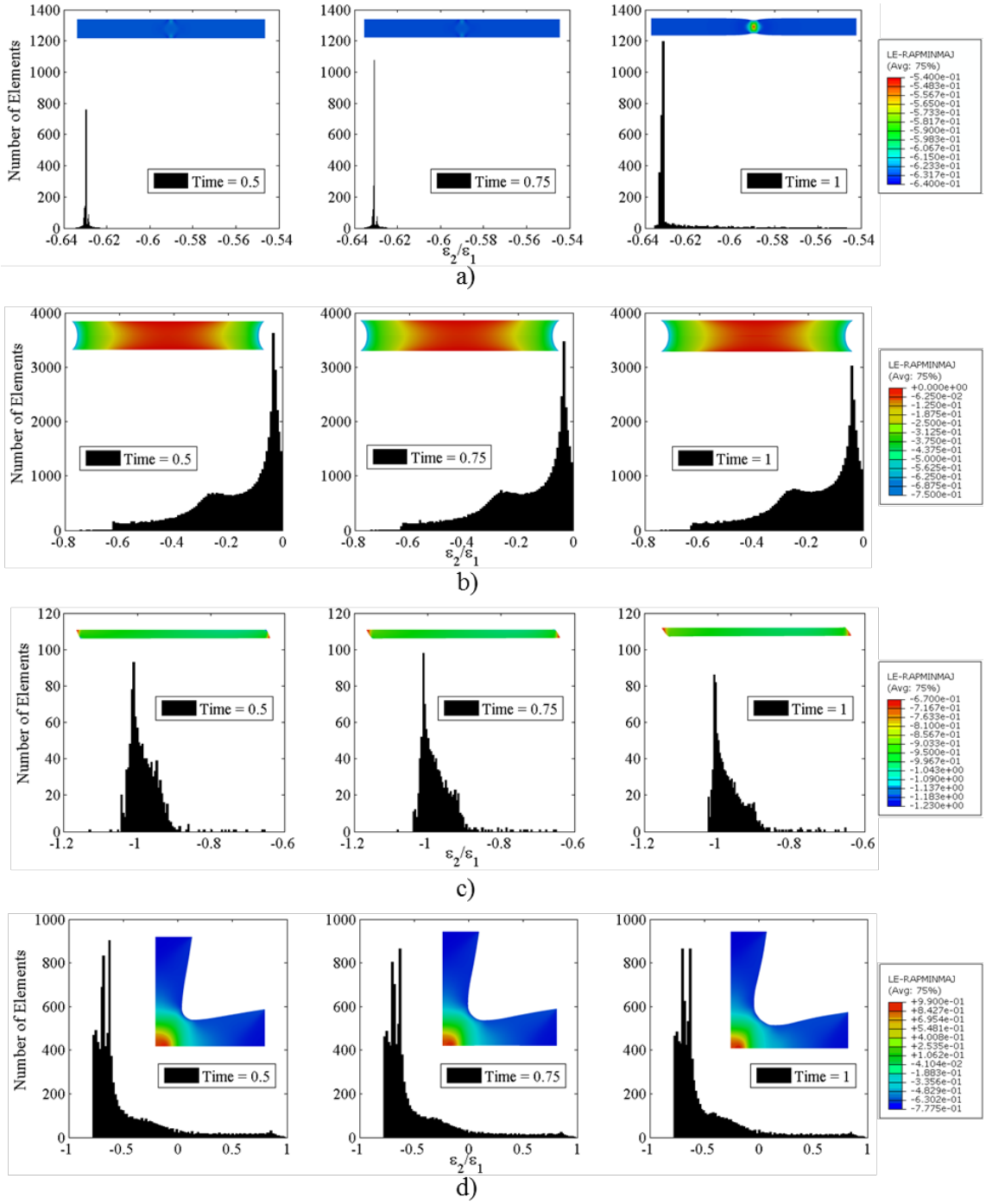

Fig. 8. Histograms representing $\varepsilon_2/\varepsilon_1$ distribution of the elements for a) uniaxial tensile, b) plane strain tension c) simple shear and d) classical biaxial test.

The TIX test is the only one covering all principal strain states, namely, uniaxial compression, shear, uniaxial, plane strain and equibiaxial tensions, as illustrated in Fig. 9 b). However, excluding uniaxial tension, the remaining strain states are localized in very small regions, as shown by $\varepsilon_2/\varepsilon_1$ contour. As for the shear-like tensile test, $\varepsilon_2/\varepsilon_1$ ratio was not calculated for some areas of TIX specimen.

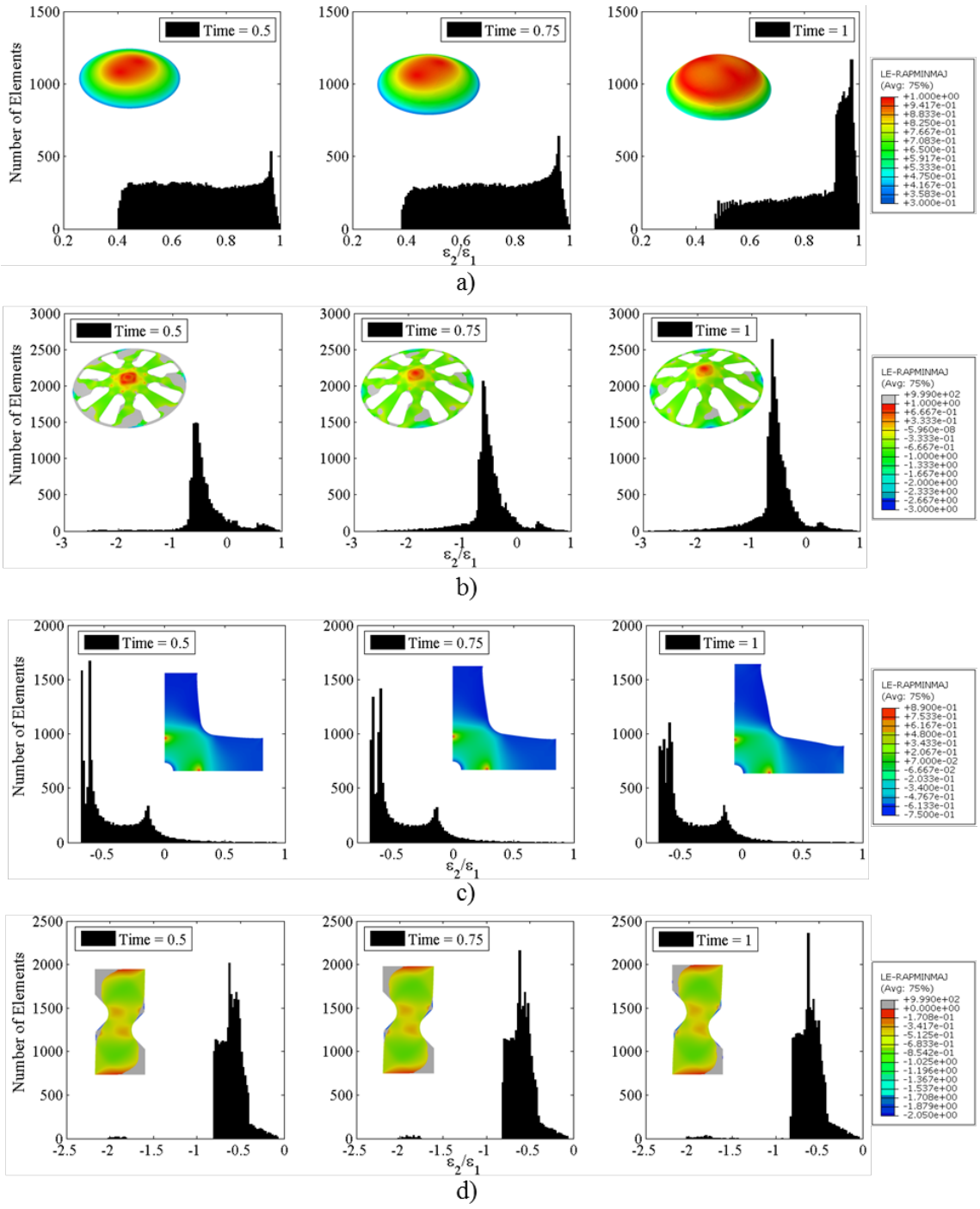

Fig. 9. Histograms representing $\varepsilon_2/\varepsilon_1$ distribution of the elements for a) bulge, b) TIX, c) biaxial tensile with hole and d) shear-like tensile test.

The evolution of $Std(\bar{\varepsilon}^{P})$ and $Std(\varepsilon_2/\varepsilon_1)$ for each test is depicted in Figs. 10 and 11. In addition, $\bar{\varepsilon}^{P}$ and $\varepsilon_2/\varepsilon_1$ evolution for all elements belonging to ROI region of the sample are included in these figures, providing supplementary information.

Analyzing $\bar{\varepsilon}^{P}$ evolution, it can be stated that, generally, a continuous increase of $Std(\bar{\varepsilon}^{P})$ occurs during the tests. The displacement imposed as boundary condition during the test leads to the specimen deformation where some regions are more deformed than the remaining ones. Consequently, a significant variation of $\bar{\varepsilon}^{P}$ on the sample may occur. In this way, the deformation heterogeneity of the specimen can be accurately measured by $Std(\bar{\varepsilon}^{P})$. An example of $Std(\bar{\varepsilon}^{P})$ functionality can be seen for the uniaxial tensile test depicted in Fig. 10 a). Due to the homogeneity of this test, $Std(\bar{\varepsilon}^{P})$ remains equal to almost zero until necking starts. However, after necking, the increase of $Std(\bar{\varepsilon}^{P})$ is verified.

In opposition, the analysis of $Std(\varepsilon_2/\varepsilon_1)$ evolution reveals that a continuous increase is not observed. Indeed, $Std(\varepsilon_2/\varepsilon_1)$ evolution tends to a stabilized value which is verified during the major part of the test. This is in agreement with the observations of Figs. 8 and 9, where it can be seen that no considerable change occurs on the covered $\varepsilon_2/\varepsilon_1$ range. Thereby, no substantial variations of $Std(\varepsilon_2/\varepsilon_1)$ value are verified during the test.

$Std(\varepsilon_2/\varepsilon_1)$ evolution is mainly influenced by the design of each test such as, for instance, the boundary conditions and specimen geometry. However, it is clear that strain localizations, such as the ones observed for uniaxial tensile (Fig. 10 a)), TIX (Fig. 11 b)) or shear-like tensile test (Fig. 11 d)), promote $Std(\varepsilon_2/\varepsilon_1)$ variation during the test.

In Figs. 12 and 13, the evolution of $(\varepsilon_2/\varepsilon_1)_{max}$, $(\varepsilon_2/\varepsilon_1)_{min}$, $\bar{\varepsilon}^{P}$ for some relevant strain states and the distribution of W_{CL} at the rupture are shown for all the tests. Note that $\bar{\varepsilon}^{P}$ value for the relevant strain states is calculated considering the elements presenting $\varepsilon_2/\varepsilon_1$ ranges depicted in Table 3. W_{CL} contours are presented in order to show the expected localization of the rupture for each test. For shear-like tensile, bulge, shear and uniaxial tensile tests, experimental and numerical rupture localization is in agreement.

Concerning the remaining tests, no experimental data is available to proceed to this kind of comparison.

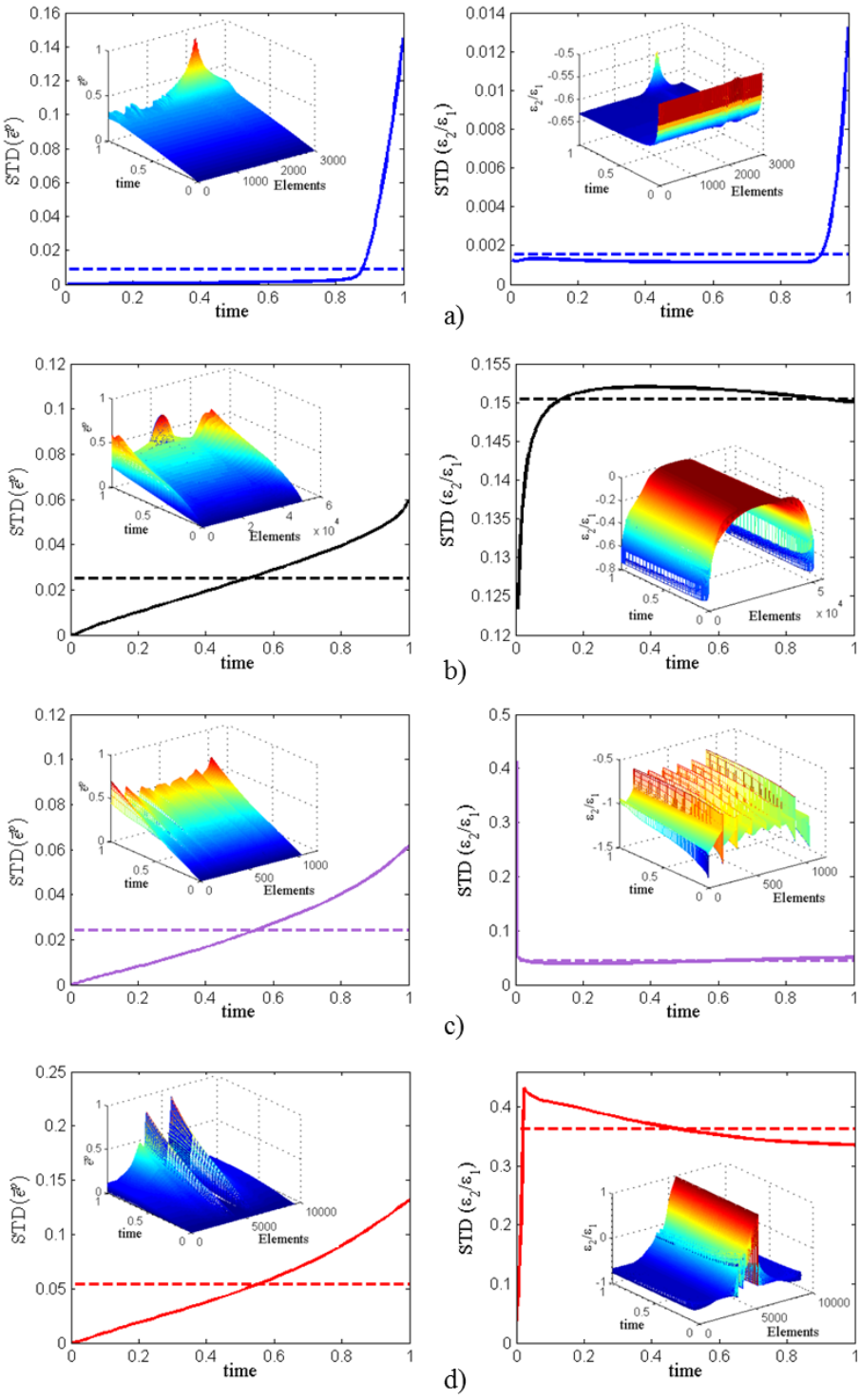

Fig. 10. Evolution of $Std(\bar{\varepsilon}^{P})$ and $Std(\varepsilon_2/\varepsilon_1)$ for a) uniaxial tensile, b) plane strain tension, c) simple shear and d) classical biaxial tensile test. The dashed lines correspond to the mean $Std(\bar{\varepsilon}^{P})$ and $Std(\varepsilon_2/\varepsilon_1)$ values.

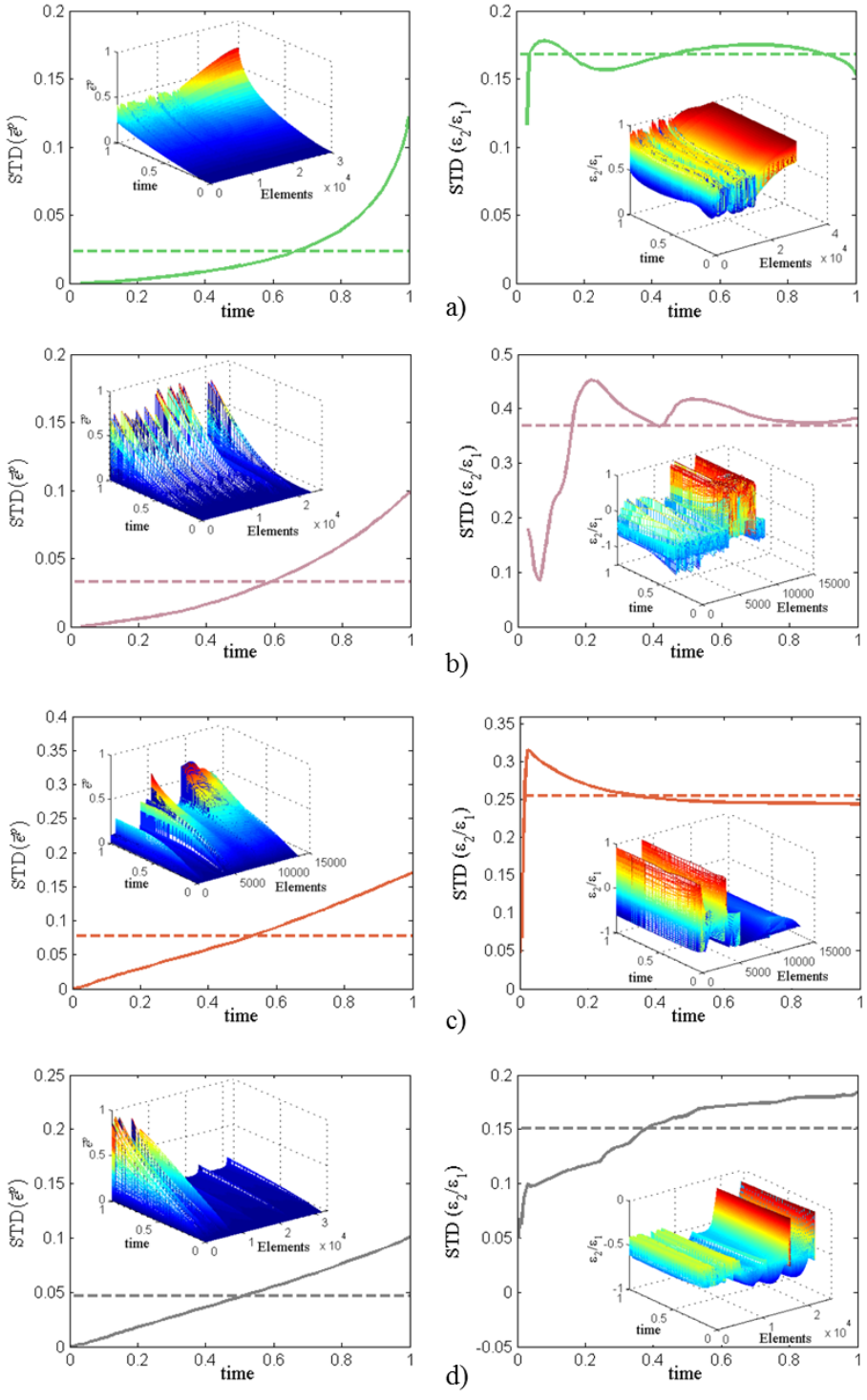

Fig. 11. Evolution of $Std(\bar{\varepsilon}^{P})$ and $Std(\varepsilon_2/\varepsilon_1)$ for a) bulge, b) TIX, c) biaxial tensile with hole and d) shear-like tensile test. The dashed lines correspond to the mean $Std(\bar{\varepsilon}^{P})$ and $Std(\varepsilon_2/\varepsilon_1)$ values.

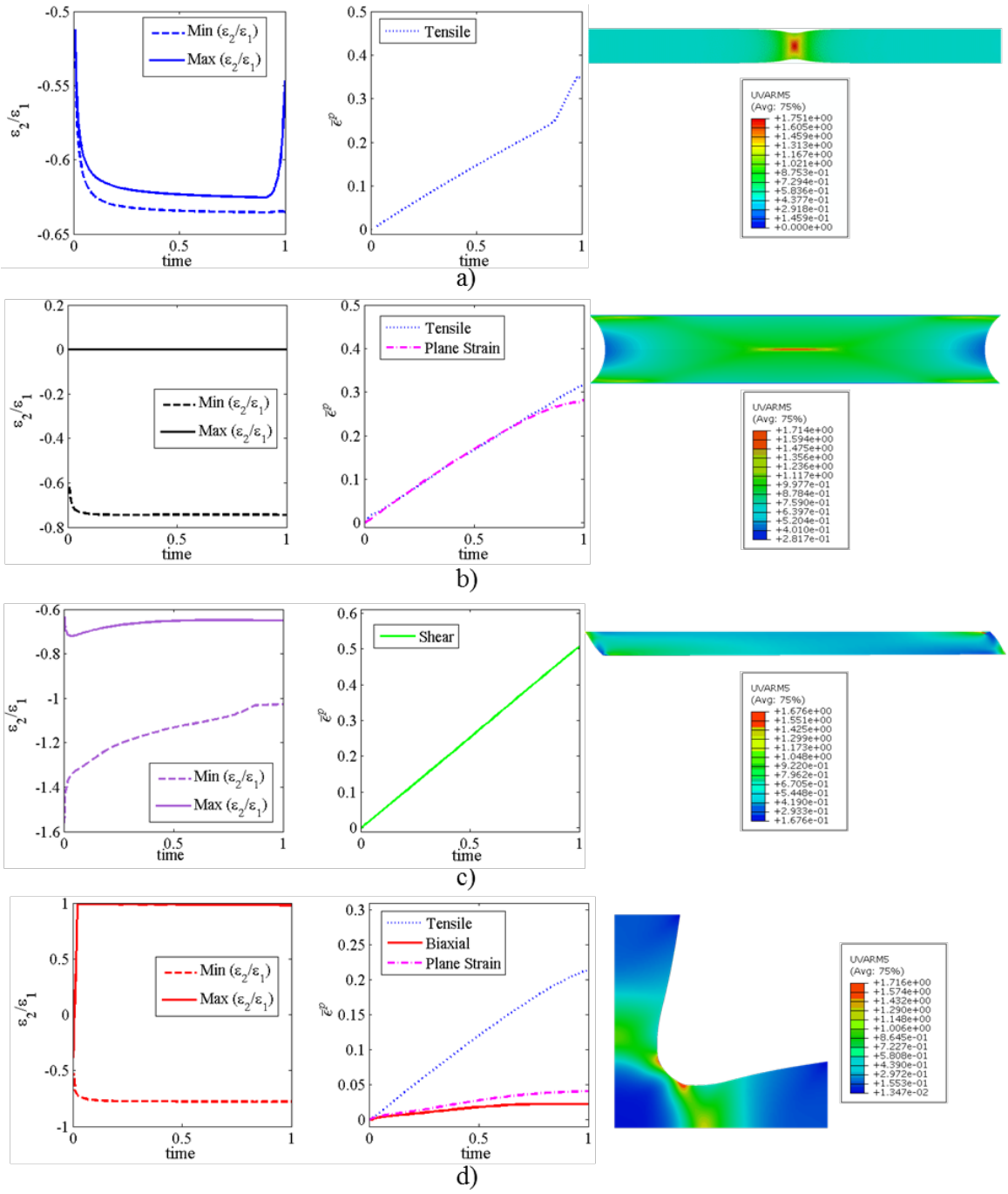

Fig. 12. Evolution of maximum and minimum $\varepsilon_2/\varepsilon_1$ values (left), maximum $\bar{\varepsilon}^{P}$ value of the different strain states (center) and W_{CL} distribution at the rupture (right) for a) uniaxial tensile, b) plane strain tension, c) simple shear and d) classical biaxial test.

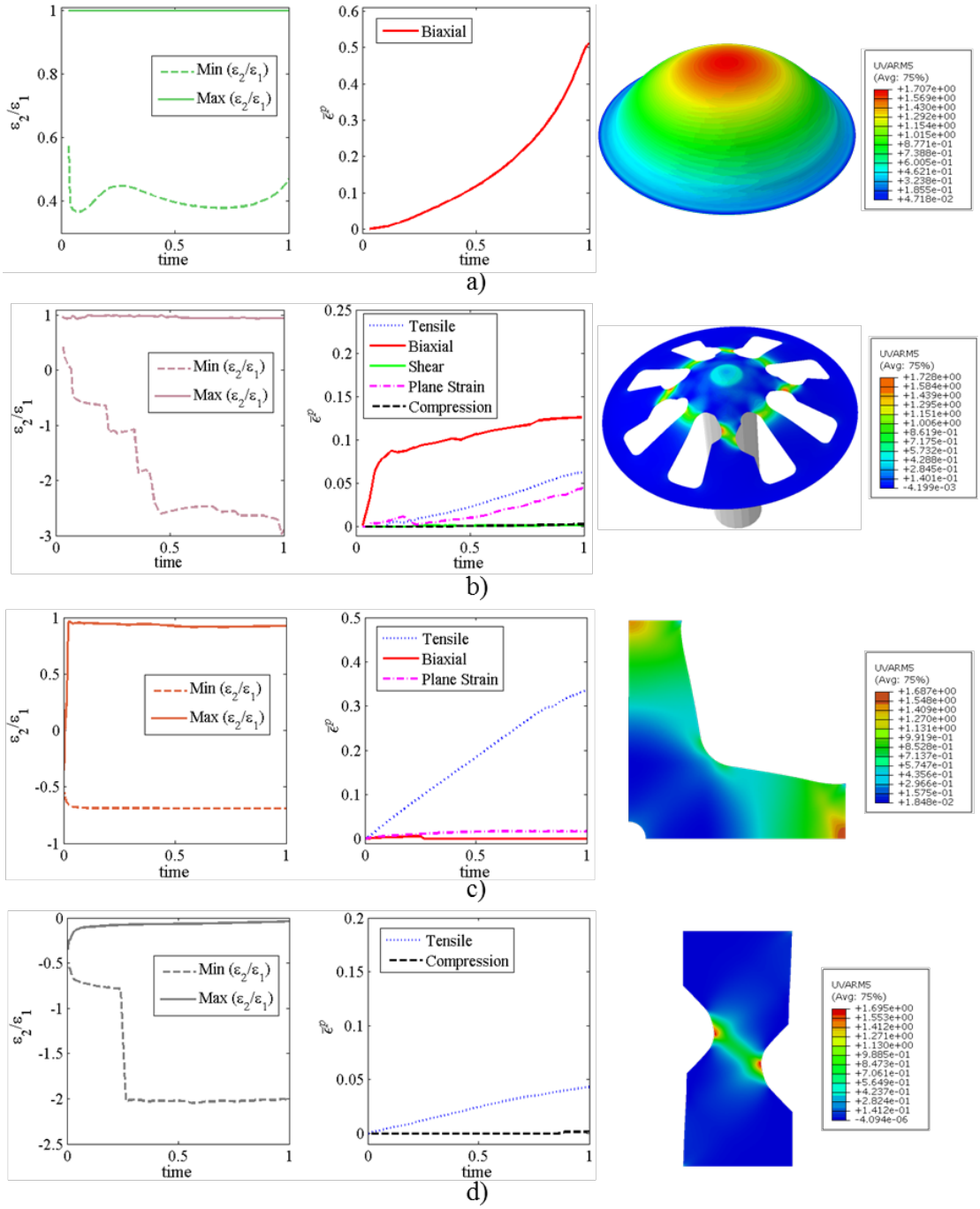

Fig. 13. Evolution of maximum and minimum $\varepsilon_2/\varepsilon_1$ values (left), maximum $\bar{\varepsilon}^P$ value of the different strain states (center) and W_{CL} distribution at the rupture (right) for a) bulge, b) TIX, c) biaxial tensile with hole and d) shear-like tensile test.

In the case of uniaxial tensile, plane strain tension, biaxial test using classical cruciform sample, bulge test and biaxial test using perforated sample (Figs. 12 a), 12 b), 12 d), 13 a) and 13 c), respectively), $(\varepsilon_2/\varepsilon_1)_{max}$ and $(\varepsilon_2/\varepsilon_1)_{min}$ values tend to be constant during the whole test.

For TIX and shear-like tensile tests (Figs. 12 c), 13 b) and 13 d), respectively), $(\varepsilon_2/\varepsilon_1)_{max}$ is constant, however, variations on $(\varepsilon_2/\varepsilon_1)_{min}$ are observed. Relatively to $(\varepsilon_2/\varepsilon_1)_{min}$ evolution for simple shear test, it can be seen that this value starts on compressive state and reaches shear strain state which is then the dominant strain state over all the specimen. In both TIX and shear-like tensile tests, the decrease of $(\varepsilon_2/\varepsilon_1)_{min}$ value during the test is due to the occurrence and evolution of compression zones in the sample.

In order to analyze the maximum and the average deformation achieved in the several tests, $\bar{\varepsilon}^{P}_{test}$ as well as $Av_{\bar{\varepsilon}^P}$ values are illustrated in Fig. 14. Concerning $\bar{\varepsilon}^{P}_{test}$, it is observed that most part of the tests achieve the same level of deformation at the end of the test. However, for $Av_{\bar{\varepsilon}^P}$, distinct values are obtained for the several tests. This is due to the fact that $Av_{\bar{\varepsilon}^P}$ is related to the overall deformation of the specimen and, depending of their design, different values are obtained at the end of each test.

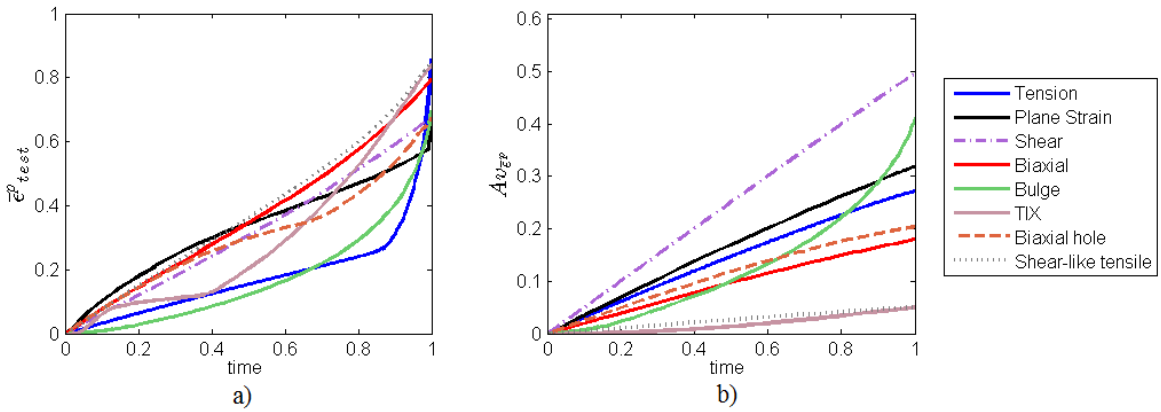

Fig. 14. Evolution of a) maximum $\bar{\varepsilon}^{P}$ value achieved during the test and b) $Av_{\bar{\varepsilon}^P}$.

Table 4 lists the values for the different contributions used in I_T formulation as well as I_T values obtained for all tests. By an individual analysis of such data, it is possible to compare directly each one of the different I_T contributions for the several tests. Based on the I_T results, a rating scale ordering the several tests by order of importance is presented in Fig. 15.

According to the proposed indicator, uniaxial tensile is the test giving the lowest information concerning the mechanical behavior of the material. This test is limited by

the small $\varepsilon_2/\varepsilon_1$ range as well as by the necking phenomenon which leads to high level of deformation only in a localized zone of the specimen.

Table 4. Obtained values for the several contributions of I_T and I_T values for the different tests.

	Tension	Plane strain	Shear	Biaxial	Bulge	TIX	Biaxial hole	Shear-like tensile
Mean Std $\varepsilon_2/\varepsilon_1$	0.001	0.150	0.044	0.363	0.168	0.369	0.255	0.151
$\left(\varepsilon_2/\varepsilon_1\right)_{\min}$	-0.636	-0.743	-1.026	-0.777	0.471	-2.898	-0.693	-2.030
$\left(\varepsilon_2/\varepsilon_1\right)_{\max}$	-0.547	0	-0.651	0.981	0.999	0.945	0.925	-0.039
Mean Std $\bar{\varepsilon}^P$	0.009	0.025	0.024	0.054	0.023	0.033	0.078	0.047
$\bar{\varepsilon}^P_{\text{test}}$	0.859	0.667	0.679	0.794	0.699	0.842	0.674	0.852
$\bar{\varepsilon}^P_{\text{tens}}$	0.348	0.317	-	0.214	-	0.063	0.336	0.043
$\bar{\varepsilon}^P_{\text{shear}}$	-	-	0.507	-	-	0.002	-	-
$\bar{\varepsilon}^P_{\text{plane}}$	-	0.283	-	0.04	-	0.046	0.017	-
$\bar{\varepsilon}^P_{\text{biaxial}}$	-	-	-	0.02	0.508	0.126	-	-
$\bar{\varepsilon}^P_{\text{comp}}$	-	-	-	-	-	0.003	-	0.001
$Av_{\bar{\varepsilon}^P}$	0.272	0.318	0.496	0.179	0.410	0.049	0.204	0.050
I_T	0.115	0.184	0.161	0.248	0.192	0.239	0.231	0.157

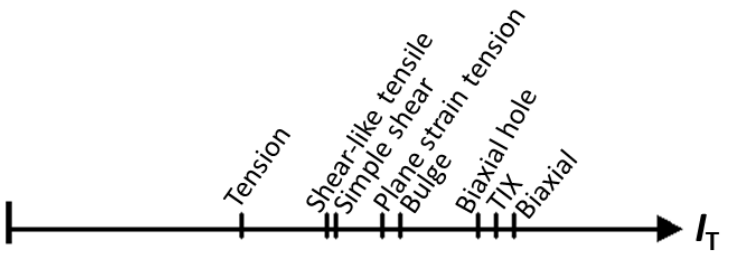

Fig. 15. Ranking of the different tests by using I_T indicator.

It can be seen that the shear-like tensile and simple shear tests provide more significant mechanical information than uniaxial tensile. Next, plane strain tension and bulge test appear providing even more mechanical information than the previous tests. It must be noted that this rating shows that plane strain tension test is much more interesting for material behavior characterization than simple shear or uniaxial tensile test. This is due to the fact that this test covers a large $\varepsilon_2/\varepsilon_1$ range with a substantial level of deformation on overall plane strain specimen.

Biaxial test using perforated sample, TIX test and biaxial test using classical cruciform specimen consist of the three tests giving a richer mechanical information. I_T indicates that biaxial tests provide more information than uniaxial ones. Indeed, these three tests are the ones covering higher $\varepsilon_2/\varepsilon_1$ range. It is interesting to note that the biaxial tensile test using classical cruciform specimen leads to a better mechanical information than the other heterogeneous tests. In fact, it must be noted that, even though TIX test was developed in order to promote shear and tensile strain in RD and TD directions as well as equibiaxial strain, small deformation levels are obtained for these strain states and for the overall specimen.

4.2. Robustness of I_T

It must be taken into account that the obtained I_T values are influenced by the relative weighting factors (w_r) adopted. Different w_r sets may change I_T rating and, therefore, a parametric study comparing three distinct w_r sets was performed in order to assess the robustness of the proposed indicator. Table 5 presents w_r sets used for this analysis.

Table 5. Different w_r sets selected for I_T robustness study.

	$I_{T\,(50\text{-}50)}$	$I_{T\,(65\text{-}35)}$	$I_{T\,(35\text{-}65)}$	
w_{r1}	0.3	0.36	0.22	Strain range/ Heterogeneity
w_{r2}	0.03	0.05	0.04	
w_{r3}	0.17	0.24	0.09	
w_{r4}	0.4	0.23	0.5	Strain level
w_{r5}	0.1	0.12	0.15	

The weighting factors w_{r1}, w_{r2} and w_{r3} are related to the I_T terms that evaluate strain state range/heterogeneity while w_{r4} and w_{r5} are related to the strain level. The three w_r sets adopted for this study consider (i) equal importance (50%-50%), (ii) 65%-35% and (iii) 35%-65% for strain range/heterogeneity and strain level, as can be seen in Table 5. It must be highlighted that $I_{T\ (50\text{-}50)}$ consists in the reference indicator calculated in the previous section.

Fig. 16 shows I_T calculations obtained for all the tests using the different w_r sets. Analyzing these results, it can be observed that the variation of w_r values leads to almost identical I_T ratings.

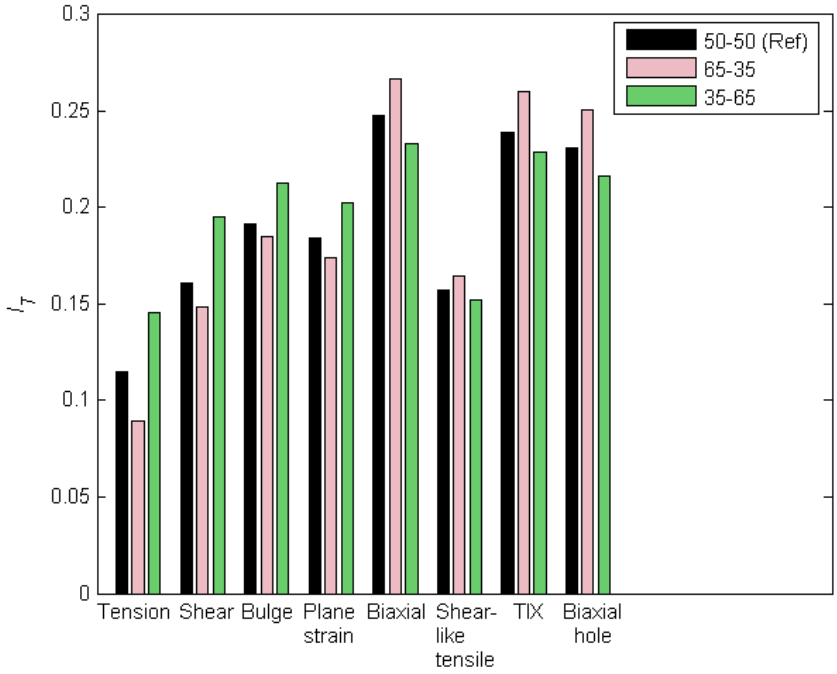

Fig. 16. I_T results obtained considering the different w_r sets.

By comparing $I_{T\ (65\text{-}35)}$ results with the reference ones ($I_{T\ (50\text{-}50)}$), it can be seen that the ranking of the several tests is quite the same, just changing the order of shear-like tensile with the simple shear test. With $I_{T\ (65\text{-}35)}$, shear-like tensile test provides some more mechanical information than simple shear. However, it must be stressed out that in the ranking obtained with the reference indicator ($I_{T\ (50\text{-}50)}$), shown in Fig. 15, no substantial difference exists between the amount of mechanical information given by these two tests since they have obtained very close $I_{T\ (50\text{-}50)}$ values. Therefore, knowing that shear-like tensile test promotes more heterogeneous strain fields than simple shear, the increase of importance of the strain state range/heterogeneity group (65%) led to the

re-ordering of these two tests. Withal, the general results suggest the achievement of similar rating when considering an I_T calculation that gives more importance to the strain range/heterogeneity contribution.

Alternatively, the comparison of the results obtained by $I_{T\ (35\text{-}65)}$ with the reference ones ($I_{T\ (50\text{-}50)}$) shows that an equal rating scale ordering the several tests is achieved. Nevertheless, it must be highlighted that the classical tests with significant level of deformation, such as bulge, plane stain or simple shear, tend to reach higher indicator values and such values became closer to the ones obtained for the better tests, namely, the TIX and the biaxial tensile tests using perforated and classical cruciform samples. Hence, it can be more difficult to distinguish the mechanical information of the several tests when a large importance to the strain achieved on the test is attributed.

According to the results obtained for the several I_T configurations tested, it can be stated that the robustness of I_T is demonstrated. Moreover, it is expected to reach a reliable reproducibility of the I_T rankings when choosing w_r values for a range comprised in-between [35% - 65%] of importance of both strain state range/heterogeneity and strain level groups. Though the w_r parameters set listed in Table 1 constitutes the standard choice, it reveals some flexibility when w_r values must be chosen. Outside of this range, I_T results tend to promote considerable changings on the ranking of the several tests.

5. Validation

With the purpose of validating the results obtained using I_T, the analysis of the material parameter sensitivity [8] of the tests was carried out. This methodology gives a comparison of the several tests, searching for the one presenting a larger sensitivity to the strain field. It should be noted that this analysis is dependent on the constitutive model, material parameter set and definition of the cost function.

5.1. Material parameter sensitivity

The material parameter sensitivity of the test expresses the sensitivity of the strain field to the parameters of the material model [8]. In this way, it is possible to evaluate the contribution of each test mainly when complex material models are used. Thus, tests with more sensitivity to the material parameters have a greater contribution on the prediction of the strain field.

As in [8], in order to quantify this sensitivity, a cost function S_{obj} is defined by the least-square difference between a reference and a perturbed data given as

$$S_{\text{obj}} = S_{\text{F}} + S_{\varepsilon_{\text{xx}}} + S_{\varepsilon_{\text{yy}}}, \tag{7}$$

with

$$S_{\text{F}} = \sqrt{\frac{1}{n_{\text{im}}}\sum_{i=1}^{n_{\text{im}}}\left(\frac{F_i(\mathbf{P}_0)-F_i(\mathbf{P})}{F_i(\mathbf{P}_0)}\right)^2}, \tag{8}$$

$$S_{\varepsilon_{\text{xx}}} = \sqrt{\frac{1}{n_{\text{im}}}\sum_{i=1}^{n_{\text{im}}}\left[\frac{1}{n_{\text{el}}}\sum_{j=1}^{n_{\text{el}}}\left(\frac{\varepsilon_{\text{xx},i,j}(\mathbf{P}_0)-\varepsilon_{\text{xx},i,j}(\mathbf{P})}{\varepsilon_{\text{xx},i,j}(\mathbf{P}_0)}\right)^2\right]} \tag{9}$$

and

$$S_{\varepsilon_{\text{yy}}} = \sqrt{\frac{1}{n_{\text{im}}}\sum_{i=1}^{n_{\text{im}}}\left[\frac{1}{n_{\text{el}}}\sum_{j=1}^{n_{\text{el}}}\left(\frac{\varepsilon_{\text{yy},i,j}(\mathbf{P}_0)-\varepsilon_{\text{yy},i,j}(\mathbf{P})}{\varepsilon_{\text{yy},i,j}(\mathbf{P}_0)}\right)^2\right]}. \tag{10}$$

where n_{im} and n_{el} are the number of strain fields and elements of the test, $F_i(\mathbf{P}_0)$ and $F_i(\mathbf{P})$ are the load values at the increment i obtained with the reference ($\mathbf{P}_0$) and the perturbed ($\mathbf{P}$) parameter set values, $\varepsilon_{\text{xx},i,j}(\mathbf{P}_0)$ and $\varepsilon_{\text{xx},i,j}(\mathbf{P})$ as well as $\varepsilon_{\text{yy},i,j}(\mathbf{P}_0)$ and $\varepsilon_{\text{yy},i,j}(\mathbf{P})$ are the strain values for the element j at the strain field i obtained using $\mathbf{P}_0$ and $\mathbf{P}$ set parameters in RD and TD directions, respectively.

Both load and strain data are taken into account on the definition of S_{obj} since it leads to a better suited solution when strain concentration and localized damage are involved [30].

Note that the sensitivity of S_{obj} to each parameter is not dependent of the reference term of S_{obj} because this term is constant. It is the perturbed term responsible to distinguish between different values of the parameter [31].

The reference parameter set $\mathbf{P}_0$ consists of the material parameters describing DC04 mechanical behavior given in Table 2, while $\mathbf{P}$ set is obtained by perturbing one of the parameters of $\mathbf{P}_0$ by -10%. Therefore, numerical simulations were carried out for all the tests perturbing individually each parameter presented in Table 2 with exception to a, $c_{44}^{(i)}$ and $c_{55}^{(i)}$, i=1,2. Hence, 24 perturbed set parameters were used on this sensitivity analysis. The reference and perturbed data were analyzed in ROI regions of the tests up to the maximum deformation level of $\bar{\varepsilon}^{P}$=0.35 by comparing 6 strain fields (n_{im}=6). The strain fields were obtained at maximum levels $\bar{\varepsilon}^{P}$= [0.1, 0.15, 0.2, 0.25, 0.3, 0.35] for each test. The sensitivity results of the cost function for the several material parameters are depicted in Figs. 17 to 19.

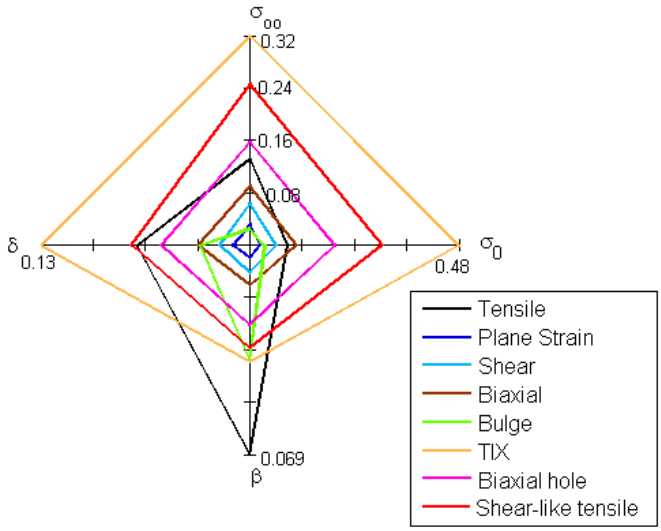

Fig. 17. Sensitivity of S_{obj} to the isotropic work hardening parameters.

Fig. 17 depicts the sensitivity of the cost function to the isotropic hardening parameters. It can be seen that the cost function is highly sensitive to the variations of σ_0 and σ_∞ while, in the case of β, the sensitivity of S_{obj} is less expressive. Among the

several tests, biaxial tensile test using perforated sample, shear-like tensile and TIX test show the greatest sensitivity to the isotropic hardening parameters.

Concerning the variations of the kinematic hardening parameters, it is verified in Fig. 18 that, generally, these material parameters lead to lower sensitivity of S_{obj} than the isotropic hardening parameters. It is justified by the fact that the contribution of the kinematic hardening is more significant when reverse strain path is considered. However, reverse strain is not verified in the tests used for this study. With exception to γ_3 and $X\text{sat}_3$ where uniaxial tensile test presents higher S_{obj} sensitivity, it is observed that biaxial test using perforated sample, shear-like tensile and TIX test show greatest sensitivity for the remaining kinematic hardening parameters. Nonetheless, a considerable difference exists between the sensitivity to the kinematic hardening parameters obtained for the TIX and the remaining mechanical tests. In order to understand the meaning of this occurrence, strain path change evolution was investigated and it was observed that some smooth strain path variation occurs in TIX test, explaining these results.

It can be stressed out that biaxial test using perforated sample, shear-like tensile and TIX test are the mechanical tests that contribute the more for the prediction of the work hardening, because these tests present strain fields with the highest sensitivity to the variations of the isotropic and kinematic hardening parameters.

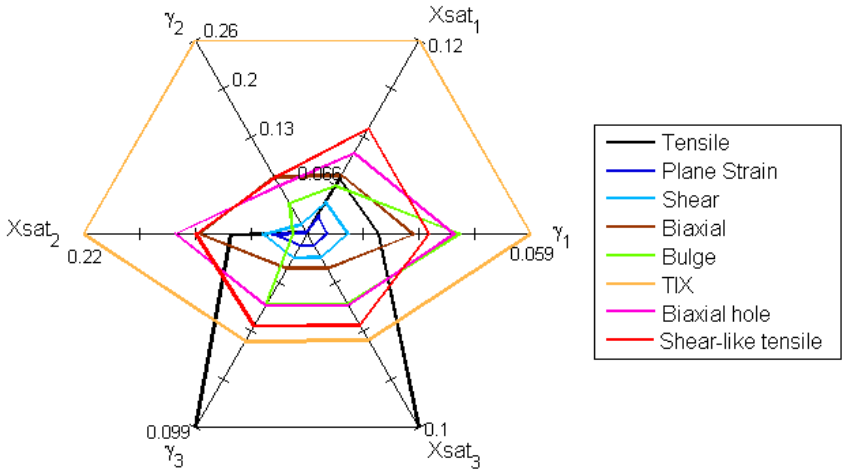

Fig. 18. Sensitivity of S_{obj} to the kinematic work hardening parameters.

The sensitivity of S_{obj} to the yield criterion parameters is illustrated in Fig. 19. It can be pointed out that the variations performed for these material parameters lead to the

major variations of the strain field due to the larger S_{obj} values obtained. In this way, these results highlight the large influence of the coefficients of *Yld2004-18p* anisotropic yield criterion on the prediction of the strain field. In addition, it is verified that TIX test as well as both biaxial tensile tests are the ones most sensitive to the anisotropy of the material since they present higher S_{obj} values. Thereby, concerning the large diversity of strain paths required by *Yld2004-18p* yield criterion it seems clear that these tests are the most indicated to characterize larger strain state ranges.

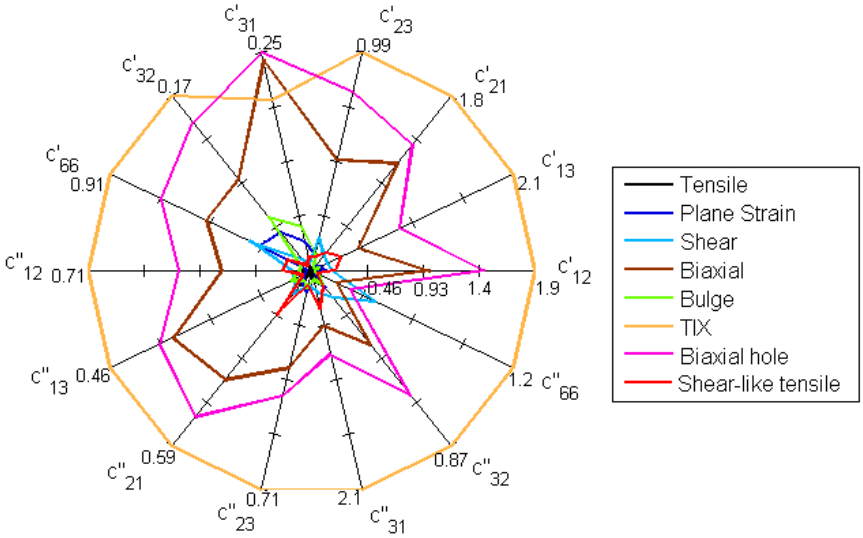

Fig. 19. Sensitivity of S_{obj} to the yield surface parameters.

The global evaluation of the results shows that TIX is the most sensitive test to the mixed work hardening as well as material anisotropy. Therefore, the material parameters sensitivity carried out indicates that this test is one of the tests that can larger contribute the prediction of the material model adopted. In part, it is due to the fact that TIX experiment develops a considerable number of the strain fields used for identifying the input parameters of this constitutive model, for instance, uniaxial tensile and simple shear at 0° and 90° to RD and also biaxial tensile state. Despite, it can be stated that a general agreement is observed between the results obtained by the validation study and by the proposed indicator. Both methodologies pointed out the same three tests (TIX and both biaxial tensile tests) as the better ones promoting the mechanical behavior characterization of the material.

On one hand, by a qualitative analysis of the mechanical tests, it seems clear that the tests involving multiaxial stresses as well as larger heterogeneity must provide a

better mechanical characterization of the material behavior. On the other hand, since the material model adopted to reproduce the DC04 mild steel behavior corresponds to a complex phenomenological model based on several stress states as well as mechanical phenomena, it seems evident that the sensitivity of the material parameters reflects the ability of the tests in reproducing these several stress states and mechanical phenomena.

6. Conclusions

A quantitative indicator able to distinguish, rate and rank mechanical tests is proposed. This indicator, called I_T, is designed to include the analysis of strain state range covered by the test, the deformation heterogeneity of the specimen as well as the strain level achieved up to rupture. For that, a continuous evaluation of the strain field up to rupture was considered.

One of the main advantages of I_T is the fact that all its contributions have physical meaning. These terms are based on strain deformations and, in addition, can be calculated experimentally by using FFM techniques.

In order to evaluate the performance of I_T, classical mechanical tests as well as modern heterogeneous tests were carried out numerically reproducing the virtual behavior of DC04 mild steel. The several I_T terms were calculated for each test and a ranking of all the tests was defined. The qualitative analysis of the mechanical tests adopted indicates that the tests involving multiaxial stresses as well as larger heterogeneity provide a more complete mechanical characterization of sheet metals. The I_T ranking obtained confirmed this trend and it revealed that the indicator proposed is able to perform an accurate quantification of the mechanical information provided by the tests. Moreover, the robustness of the I_T results was also investigated and identical ratings ordering the several tests were achieved.

With the purpose of comparing results and validate I_T, a material parameter sensitivity study was performed. In this analysis, a cost function was defined based on load and strain data for each test and the sensitivity of the strain field was evaluated by perturbing each material parameter. According to the obtained results as well as its validation, it was shown that the proposed indicator consists of an efficient strategy for

choosing the more appropriate heterogeneous test when it comes to identification of material properties. Future work will deal with applying the proposed indicator on the design of innovative heterogeneous mechanical tests promoting a better material behavior characterization of the sheet metals.

Acknowledgements

The authors would like to acknowledge the Région Bretagne (France) for its financial support. This work was also co-financed by the Portuguese Foundation for Science and Technology via project PTDC/EME-TME/118420/2010 and by FEDER via the "Programa Operacional Factores de Competitividade" of QREN with COMPETE reference: FCOMP-01-0124-FEDER-020465. One of the authors, N. Souto, was also supported by the grant SFRH/BD/80564/2011 from the Portuguese Science and Technology Foundation. All supports are gratefully acknowledged.

References

[1] A. Andrade-Campos, S. Thuillier, P. Pilvin, F. Teixeira-Dias, On the Determination of Material Parameters for Internal Variable Thermoelastic–Viscoplastic Constitutive Models, International Journal of Plasticity, 23 (2007) 1349-1379.

[2] B.M. Chaparro, S. Thuillier, L.F. Menezes, P.Y. Manach, J.V. Fernandes, Material parameters identification: Gradient-based, genetic and hybrid optimization algorithms, Computational Materials Science, 44 (2008) 339–346.

[3] F. Barlat, H. Aretz, J.W. Yoon, M.E. Karabin, J.C. Brem, R.E. Dick, Linear transfomation-based anisotropic yield functions, International Journal of Plasticity, 21 (2005) 1009–1039.

[4] F. Bron, J. Besson, A yield function for anisotropic materials application to aluminum alloys, International Journal of Plasticity, 20 (2004) 937–963.

[5] H. Vegter, A.H.v.d. Boogaard, A plane stress yield function for anisotropic sheet material by interpolation of biaxial stress states, International Journal of Plasticity, 22 (2006) 557-580.

[6] F. Yoshida, H. Hamasaki, T. Uemori, A user-friendly 3D yield function to describe anisotropy of steel sheets, International Journal of Plasticity, 45 (2013) 119–139.

[7] M. Grédiac, The use of full-field measurement methods in composite material characterization: interest and limitations, Composites: Part A, 35 (2004) 751–761.

[8] S. Belhabib, H. Haddadi, M. Gaspérini, P. Vacher, Heterogeneous tensile test on elastoplastic metallic sheets: Comparison between FEM simulations and full-field strain measurements, International Journal of Mechanical Sciences, 50 (2008) 14–21.

[9] S. Cooreman, Identification of the plastic material behaviour through full-field displacement measurements and inverse methods, in, Vrije Universiteit Brussel, Belgium, 2008.

[10] A. Güner, C. Soyarslan, A. Brosius, A.E. Tekkaya, Characterization of anisotropy of sheet metals employing inhomogeneous strain fields for Yld2000-2D yield function, International Journal of Solids and Structures, 49 (2012) 3517-3527.

[11] H. Haddadi, S. Belhabib, Improving the characterization of a hardening law using digital image correlation over an enhanced heterogeneous tensile test, International Journal of Mechanical Sciences, 62 (2012) 47-56.

[12] J. Kajberg, G. Lindkvist, Characterisation of materials subjected to large strains by inverse modelling based on in-plane displacement fields, International Journal of Solids and Structures, 41 (2004) 3439–3459.

[13] M.H.H. Meuwissen, An inverse method for the mechanical characterisation of metals, in, Eindhoven University of Technology, Netherlands, 1998.

[14] M.H.H. Meuwissen, C.W.J. Oomens, F.P.T. Baaijens, R. Petterson, J.D. Janssen, Determination of the elasto-plastic properties of aluminium using a mixed numerical–experimental method, Journal of Materials Processing Technology, 75 (1998) 204–211.

[15] T. Pottier, P. Vacher, F. Toussaint, Contribution of heterogeneous strain field measurements and boundary conditions modelling in inverse identification of material parameters, European Journal of Mechanics A/Solids, 30 (2011) 373-382.

[16] S. Cooreman, D. Lecompte, H. Sol, J. Vantomme, D. Debruyne, Identification of Mechanical Material Behavior Through Inverse Modeling and DIC, Experimental Mechanics 48 (2008) 421–433.

[17] M. Teaca, I. Charpentier, M. Martiny, G. Ferron, Identification of sheet metal plastic anisotropy using heterogeneous biaxial tensile tests, International Journal of Mechanical Sciences, 52 (2010) 572–580.

[18] I. Zidane, D. Guines, L. Léotoing, E. Ragneau, Development of an in-plane biaxial test for forming limit curve (FLC) characterization of metallic sheets, Measurement Science and Technology, 21 (2010) 1-11.

[19] T. Pottier, P. Vacher, F. Toussaint, H. Louche, T. Coudert, Out-of-plane Testing Procedure for Inverse Identification Purpose: Application in Sheet Metal Plasticity, Experimental Mechanics, (2011) 1-13.

[20] D.R. Shouler, J.M. Allwood, Design and use of a novel sample design for formability testing in pure shear, Journal of Materials Processing Technology, 210 (2010) 1304–1313.

[21] Q. Yin, A. Brosius, A.E. Tekkaya, Modified plane torsion tests for sheet metal characterization, in: Steel research international, Special edition: 10th international conference on technology of plasticity, ICTP 2011, 2011, pp. 696-701.

[22] Q. Yin, C. Soyarslan, A. Guner, A. Brosius, A.E. Tekkaya, A cyclic twin bridge shear test for the identification of kinematic hardening parameters, International Journal of Mechanical Sciences, 59 (2012) 31-43.

[23] D. Banabic, F. Barlat, O. Cazacu, T. Kuwabara, Advances in anisotropy and formability, International Journal of Material Forming, 3 (2010) 165-189.

[24] S. Bouvier, H. Haddadi, P. Levée, C. Teodosiu, Simple shear tests: Experimental techniques and characterization of the plastic anisotropy of rolled sheets at large strains, Journal of Materials Processing Technology, v.172 (2006) 96–103.

[25] N. Souto, A. Andrade-Campos, S. Thuillier, Material parameter identification within an integrated methodology considering anisotropy, hardening and rupture, Journal of Materials Processing Technology, 220 (2015) 157-172.

[26] S. Thuillier, P.Y. Manach, Comparison of the Work-Hardening of Metallic Sheets using Tensile and Shear Strain Paths, International Journal of Plasticity, 25 (2008) 733-751.

[27] R.J.A.d. Sousa, J.W. Yoon, R.P.R. Cardoso, R.A.F. Valente, J.J. Grácio, On the use of a reduced enhanced solid-shell (RESS) element for sheet forming simulations, International Journal of Plasticity, 23 (2007) 490–515.

[28] P.A. Prates, M.C. Oliveira, J.V. Fernandes, A new strategy for the simultaneous identification of constitutive laws parameters of metal sheets using a single test, Computational Materials Science, 85 (2014) 102–120.

[29] R.H. Wagoner, Comparison of Plane-Strain and Tensile Work Hardening in Two Sheet Steel Alloys, Metallurgical Transactions, 12 (1981) 877-882.

[30] S. Avril, M. Bonnet, A.-S. Bretelle, M. Grédiac, F. Hild, P. Ienny, F. Latourte, D. Lemosse, S. Pagano, E. Pagnacco, F. Pierron, Overview of Identification methods of mechanical parameters based on full-field measurements, Experimental Mechanics, 48 (2008) 381-402.

[31] R.A.F. Valente, R.A.d. Sousa, A. Andrade-Campos, J.F. Caseiro, Computational Methods in Metal Forming Simulation - Finite Element Formulations and Optimization Strategies, Springer, 2014.